

DC-DC 4-Switch Buck-Boost Converter for Energy Harvesting from Elliptical Machines

by

Alexander Samietz

Gustavo Guzman

Senior Project

Electrical Engineering Department

California Polytechnic State University

San Luis Obispo

2018

# TABLE OF CONTENTS

<i>Section</i>	<i>Page</i>
Abstract.....	1
Chapter 1: Introduction.....	2
Chapter 2: Customer Needs, Requirements, and Specifications.....	3
1. Customer Needs Assessment.....	3
2. Requirements and Specifications.....	3
Chapter 3: Functional Decomposition.....	6
Chapter 4: Project Planning.....	8
Chapter 5: Circuit Design and Simulations.....	11
Chapter 6: Component Selection and PCB Layout.....	26
Chapter 7: Assembly.....	41
Chapter 8: Testing.....	42
Chapter 9: Future Plans and Takeaways.....	43
Bibliography.....	44
<i>Appendices</i>	
A. Senior Project Analysis.....	47
B. LTSpice .net File .....	51

## Lists of Tables and Figures

<i>TABLES</i>	<i>Page</i>
Table I. DC-DC Buck-boost Converter Requirements & Specifications.....	4
Table II. DC-DC Buck-boost Converter Project Deliverables.....	5
Table III. Level 0 DC-DC Buck-boost converter Functional Requirement.....	6
Table IV. Level 1 DC-DC Buck-boost converter Functional Requirement.....	7
Table V. DC-DC Buck-boost converter Cost Estimates.....	9
Table VI. Summary of Actual Project Costs.....	10
Table VII. Maximum ratings for MOSFETs BSZ100N06IS3G.....	13
Table VIII. Maximum Voltage Ratings for the Four External Switches Based on Simulation	14
Table IX. BSZ100N06LS3G NMOS Specifications.....	26
 <i>FIGURES</i>	
Figure I. Level 0 DC-DC Buck-boost Converter Block Diagram.....	6
Figure II. Level 1 DC-DC Buck-boost Converter Block Diagram.....	6
Figure III. EE 460, EE 461, and EE 462 Gantt Charts.....	8
Figure IV. LT8390 Test Fixture Schematic.....	11
Figure V. Safe Operating Area of the N-channel MOSFET BSZ100N06LS3G.....	14
Figure VI. 36 V output voltage, < 1 V output voltage ripple with 0.277 Electronic load.....	16
Figure VII. Boost region inductor current waveform using electronic load.....	16
Figure VIII. $V_{DS}$ waveforms for four external MOSFET switches using electronic load.....	17
Figure IX. 36 V output voltage, <1 V output voltage ripple with 130 $\Omega$ resistive load.....	17
Figure X. Boost region inductor current waveform using a resistive load.....	18
Figure XI. $V_{DS}$ waveforms for four external MOSFET switches using a resistive load.....	18
Figure XII. 36 V output voltage, <1 V output voltage ripple with 5.4 A electronic load.....	19
Figure XIII. Buck region inductor current waveform using electronic load.....	19
Figure XIV. $V_{DS}$ waveforms for the four external MOSFET switches using electronic load...	20
Figure XV. 35.61 V output voltage, <1 V output voltage ripple with 5.3 $\Omega$ resistive load.....	20
Figure XVI. Buck region inductor current waveform using a resistive load.....	21
Figure XVII. $V_{DS}$ waveforms for the four external MOSFET switches using a resistive load...	21

Figure XVIII. 36.19 V output voltage, <1 V output voltage ripple with 3.7 A electronic load	22
Figure XIX. Buck-boost region inductor current waveform using an electronic load.....	23
Figure XX. $V_{DS}$ waveforms for the four external MOSFET switches using an electronic load	23
Figure XXI. 36.19 V output voltage, <1 V output voltage ripple with 10 $\Omega$ resistive load....	24
Figure XXII. Buck-boost region inductor current waveform using a resistive load.....	24
Figure XXIII: $V_{DS}$ waveforms for the four external MOSFET switches using a resistive load	25
Figure XXIV. Schematic for First Revision of Board.....	27
Figure XXV. Front Layer for First Revision of Board.....	28
Figure XXVI. Back Layer for First Revision of Board.....	29
Figure XXVII. Schematic for Second Revision of Board.....	31
Figure XXVIII. Front Layer for Second Revision of Board.....	32
Figure XXIV. Back Layer for Second Revision of Board.....	33
Figure XXX. Front Layer for Third Revision of Board.....	34
Figure XXXI. Back Layer for Third Revision of Board.....	35
Figure XXXII. Schematic for Final Revision of Board.....	37
Figure XXXIII. Front Layer for Final Revision of Board.....	38
Figure XXXIV. Back Layer for Final Revision of Board.....	39
Figure XXXVI. Final soldered PCB.....	41

## **Abstract**

The senior project report documents the process of replacing the network of resistors inside an elliptical machine with a DC-DC buck-boost converter. The buck-boost DC-DC converter accepts a wide input range of 5-60 Volts, with an output of 36 Volts for the most efficient use of the already available microinverter. The microinverter reclaims the lost energy and safely distributes it back to the electrical grid. The addition of this project reduces heat emissions from wasted energy and shrinks the carbon footprint of its users.

## Chapter 1: Introduction

This project intends to provide a solution to the wasted, unused energy produced by the Precor elliptical workout machine. The Cal Poly recreation center currently houses dozens of Precor elliptical machines all capable of harnessing lost energy. The opportunity for an entity to develop a process that harnesses the energy relates ideally to the Energy Harvesting from Exercise Machines project at Cal Poly. The project focuses on the DC-DC converter. The DC-DC converter stabilizes the sporadic and unpredictable elliptical output and converts the output to a desired input voltage for the microinverter. The project undergoes the design, testing, and revision process of the DC-DC converter that achieves maximum efficiency.

Professor Braun first conceived this idea in 2007 and has produced multiple projects since its inception [1]. This report takes advantage of a relatively new buck/boost controller developed by Linear Technology. The controller has a large input range of 4-60 Volts, precisely the voltage range produced by an elliptical machine. Efficiency of the controller exceeds 90% for its complete input range, allowing for minimal energy loss. [2-4]. A pre-purchased microinverter reduces project complications. This report references work done by a previous student at Cal Poly, Angelo Gallardo, who used the same controller in his master's thesis [5] and Andrew Forster who developed a four-switch buck-boost DC-DC converter [5,6].

Currently, several companies provide solutions to the problem mentioned above. For example, The Green Revolution and ReSource Fitness manufacture entirely new devices including an internal energy harvester [7]. ReRev retrofits old exercise machines that harness the energy. ReRev has outfitted old machines at over 28 universities across the U.S. [8]. The high demand for energy harvesting machines creates an abundant opportunity for development. However, an investment return for consumers takes a long time before benefits show. By producing a more efficient, cost friendly solution, not only do investors earn their money back quicker, but the environment sees a positive, sustainable impact.

The elliptical machines work by submitting the user to physical resistance using a magnetic synchronous generator. The more resistance, the more current the magnetic generator produces, thus creating a harder workout for the user [9]. The rectified AC voltage, through a network of resistors dissipates as heat. Intervening in this process and replacing the network of resistors with a DC-DC generator mentioned above, creates an opportunity to harness wasted energy.

Cal Poly's attempt at harnessing unused energy in previous years had minimal success. This included purchasing off-the-shelf DC-DC converters and interfacing with the elliptical machines. The efficiency of the converters topped off at about 40%, but at higher power levels the converter failed [4]. As a result, the project necessitates making the converter more efficient than previous attempts. This report documents the design process and provides the results. To determine what to design, the customer's needs, requirements, and specifications were investigated.

## **Chapter 2: Customer Needs, Requirements, and Specifications**

This chapter highlights the customer needs and marketing requirements important to the design process of the system.

### **Customer Needs**

The intended customers for this product consist of gym owners or those who have a personal gym. To elicit the customer needs, interviews were conducted with those who consider themselves environmentalists. This included gym regulars and an environmental engineer. When purchasing the product, the customer reiterated the goal of sustainability thinking. The product's major appeal to consumers is the system's ability to harvest wasted energy from a machine and turn it into usable, reliable energy. Any process that makes the product more effective, the more the consumer wants it. A customer need that overshadows the project stems from project price. A customer would refuse to purchase the product, if the system does not guarantee an investment return, meaning the product pays itself off before the end of the products lifecycle. Minimizing the system's power needs would guarantee the consumer's investment is returned. Designing the product that allowed consumer installation within the elliptical machine reduces cost. Requiring the device to fit inside the elliptical machine would remove extra casing needed. Easy installation would save the customer money by avoiding a professional for proper installation. The most important need, especially to the Recreation Center, is safety. The Recreation Center has strict guidelines regarding safety due to the vast number of users it sees every day. No matter the performance of the machine, if it is not safe it will not be purchased. The design process will emphasize this.

### **Marketing Requirements and Specifications**

The requirements and specifications change based on customer needs, and technical and performance constraints. Adding unnecessary costs to the product would reduce its viability for potential customers. For example, adding extra casing or having extra installation steps would scare customers away, potentially to a competitor's product that avoids unnecessary costs and extra installation steps. Cost is also an important system consideration. The product should pay itself back before the end of its lifecycle, so having a cost higher than the savings produced by the product would make it unviable. Designing the product to work on different exercise machines would not only produce more energy for the consumer, but also would expand the customer-base. Lastly, the product's overarching theme focuses on efficiency. The product should achieve higher efficiency than previous related projects [6]. If the system consumes more power than it produces, then it defeats the purpose of the project.

Table I below shows marketing requirements, engineering specifications, and justifications.

TABLE I  
DC-DC BUCK-BOOST CONVERTER REQUIREMENTS AND SPECIFICATIONS

Marketing Requirements	Engineering Specifications	Justification
4,5	Output 36 Volts within $\pm 1.8$ Volts of the desired value and output a current no more than 8 Amps.	36 Volts achieves highest efficiency for the purchased microinverter [5]. Allowing for the highest efficiency reduces product waste.
5	Operates with a DC-DC controller efficiency of 90% or greater over the input voltage range.	To recoup production costs, the project requires high efficiency, which allows the user to maximize money savings.
4,5	Accepts a voltage range of 5-60 Volts and accept an input current no more than 4 Amps.	Depending on the user and intensity of the workout, the voltage produced varies. The micro inverter takes a max input current of 7 A [4].
1	The system must meet all UL 1741 and IEEE 1547 requirements.	These requirements protect the grid, keep the system safe, reliable and environmentally responsible.
1,2	Fits within a 7"x7"x4" rectangular volume, weigh less than 1 kg, and fit inside the elliptical	Should not have to add extra casing which would add unnecessary cost to the system. Having the controller and converter outside of the machine could cause congested areas around it.
3	Production cost less than \$360.	Production cost comes from conservative estimate of 100W workout, with 90% inverter efficiency, DC-DC converter efficiency of 80%, and 12 hours of machine use per day for 41 weeks out of a year [10]. If the system doesn't generate money, or break even, over the product lifetime's course, then no monetary reason to use it.
3,5	Connectors should use spade lugs to connect to the elliptical machine and banana plugs to connect to the DCDC converter [4].	Familiar connectors allow for quick and easy installation [5].
<b>Marketing Requirements</b>		
1. Safety		



- |   |
|---|
| <ol style="list-style-type: none"> <li>2. Small and compact</li> <li>3. Low-cost</li> <li>4. Versatile</li> <li>5. Efficient</li> </ol> |
|---|

Table II below shows the deliverables and their corresponding due dates. The next chapter deals with the functional decomposition of the system.

TABLE II  
DC-DC BUCK-BOOST CONVERTER DELIVERABLES

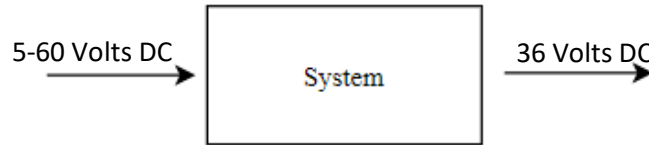
Delivery Date	Deliverable Description
April 16th	Design Review
June 14th	EE 461 report
June 14th	First Version of Board Layout
December 6th	EE 462 demo
	ABET Sr. Project Analysis
	Sr. Project Expo Poster
December 15th	EE 462 Report

Chapter 3 goes into detail about the high level and low level functional decompositions. This structure allows an easy-to-follow process of how the system works.

### Chapter 3: Functional Decomposition

To have a grasp in the macro and micro levels to which this system is being designed, multiple block diagrams are created to map out different levels of the design.

Figure 1 shows the level 0 block diagram for the system.



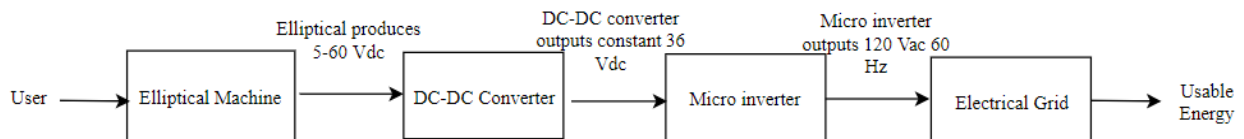
**Figure I:** Level 0 Energy DC-DC Buck-Boost Converter Block Diagram.

Table III shows level 0 system functional requirements. The user pedals an existing elliptical machine at different speeds, producing a range of voltages. The system converts the voltage range into usable energy that’s delivered to the grid at 120 Vac, 15A and 60 Hz.

TABLE III:  
DC-DC BUCK-BOOST CONVERTER FUNCTIONAL REQUIREMENTS

Module	System
Input	Gym user pedaling elliptical machine at variable speeds producing 5-60 Vdc
Output	Regulated 36 Vdc
Function	The user utilizing the elliptical machine produces voltages of 5-60 volts. A device captures the energy and converts it to an acceptable 36 volts for the micro inverter, which delivers it safely to the grid.

In Figure II, the level 1 block diagram shows the basic inputs and outputs for the EHFEM project. The level 1 architecture contains the elliptical machine operated by a user, DC-DC converter, micro inverter, and the electrical grid. The elliptical machine produces 5-60 Vdc that feeds into the DC-DC Converter, which steps down or up the input voltage to a constant 36 Vdc output voltage. The micro inverter takes the 36 Vdc output voltage and inverts it to 120Vac at 60 Hz.



**Figure II:** Level 1 EHFEM Block Diagram

Table IV shows level 1 functional requirements, which contain all subsystems. Each module has inputs, corresponding outputs, and main functions. The level 1 architecture consists of the user, elliptical machine, DC-DC converter, micro inverter, and the electrical grid.

TABLE IV:  
DC-DC BUCK-BOOST CONVERTER FUNCTIONAL REQUIREMENTS

Module	Elliptical Machine	DC-DC Converter	Micro inverter	Electrical Grid
Input	User	DC Voltage range 5-60 V	Constant 36 Vdc below 7A	120 Vac at 15 A and 60 Hz
Output	DC Voltage range 5-60 V	Constant 36 Vdc below 7 A	120 Vac 60 Hz at 15 A	Usable Energy
Functionality	Converts physical movement into DC voltages	Steps up/down the input voltage into constant output voltage	Converts output voltage into 120 Vac at 15 A and 60 Hz	Delivers power

Chapter 4 goes into detail about the projects schedule, laying out a plan for deadlines to be met. Working out the projects schedule provides a timeline for the delivery of necessary components.

## Chapter 4: Project Planning

This chapter highlights the timing and costs of the project and its planning. Figure 3 shows the timeline project using a Gantt chart. The project timeline separates into three senior project classes which allow two designs, build, and test iterations with the final iteration due week eight of fall quarter. 461 and 462 include assigned individual tasks. The final figure represents the actual timeline which transpired to date.

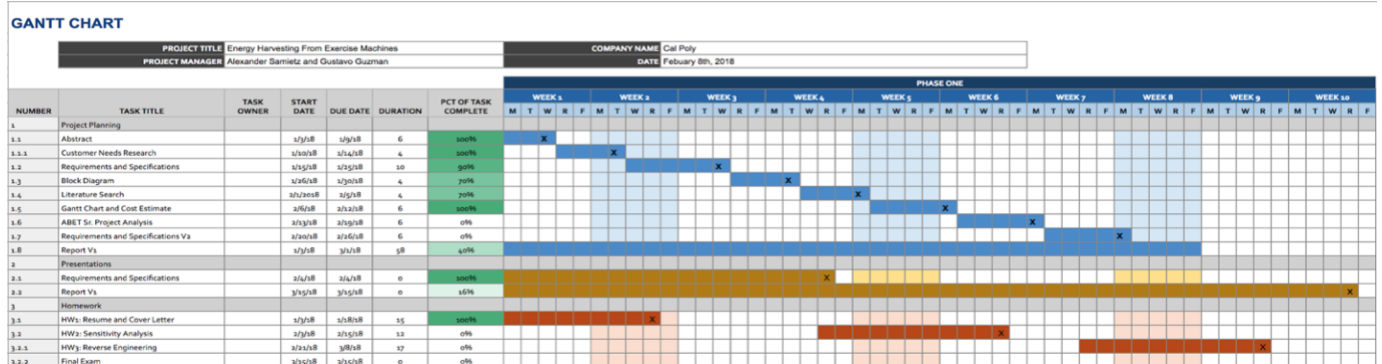


Figure IIIa: EE 460 Gantt Chart

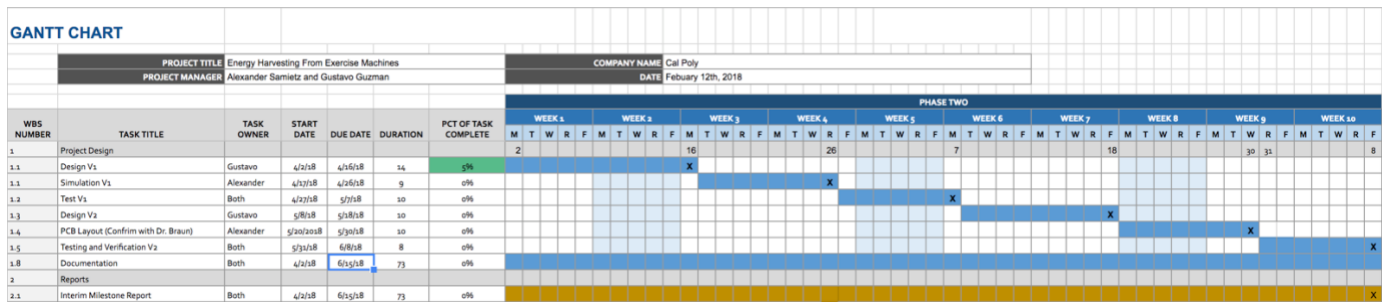


Figure IIIb: EE 461 Gantt Chart

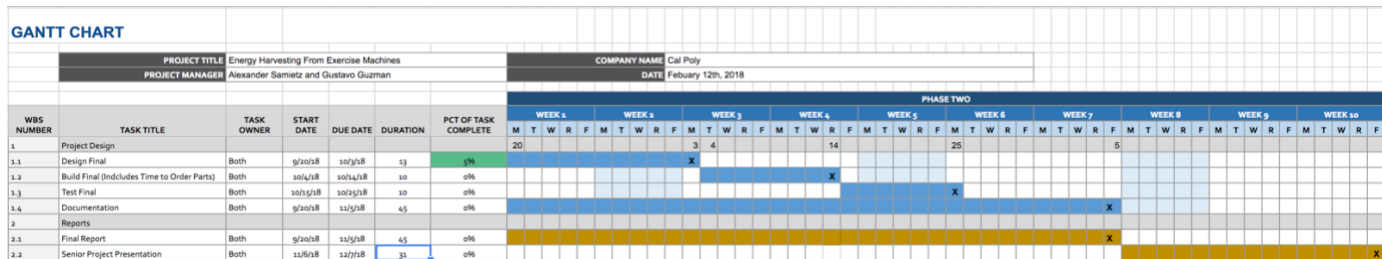


Figure IIIb: EE 462 Gantt Chart

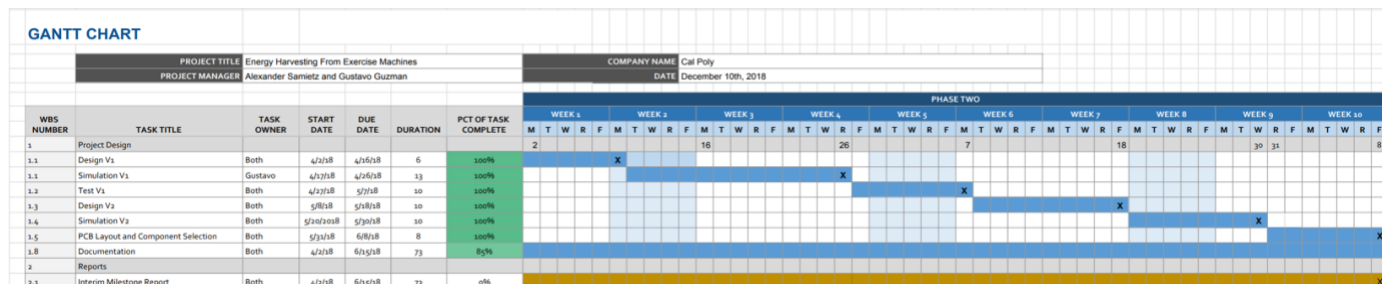


Figure IIIc: EE 461 Actual Gantt Chart

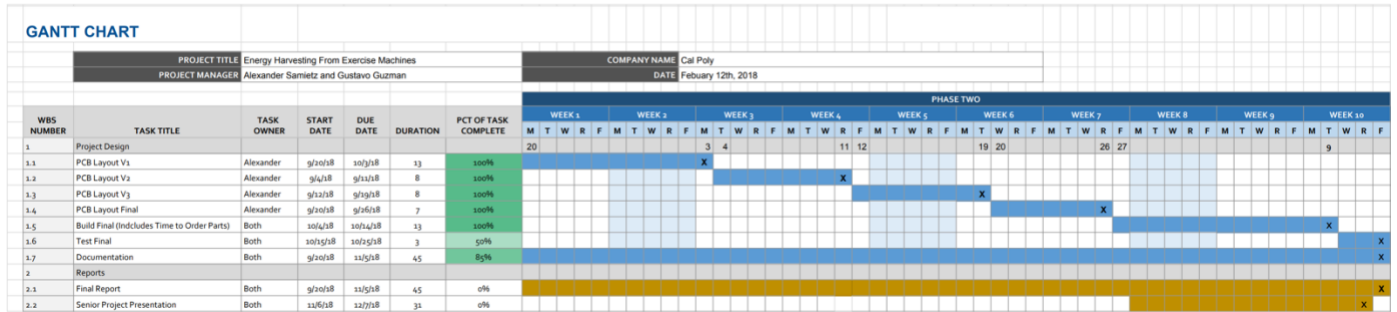


Figure III: EE 462 Actual Gantt Chart

The cost of the project can be estimated using three different measures of cost: most optimistic, most likely, and most pessimistic. These are averaged to find the most likely cost. This was done with time duration to find the most likely amount of hours to complete the project.

$$Cost = \frac{cost_{most\ optimistic} + 4cost_{most\ likely} + cost_{most\ pessimistic}}{6} = \frac{20,000 + 92,000 + 26,000}{6} = \$23,000 \quad (1)$$

$$Expected\ Time = \frac{T_o + 4T_m + T_p}{6} = \frac{100 + 600 + 200}{6} = 150\ hours \quad (2)$$

TABLE V  
SUMMARY OF PROJECT COSTS

Item	Cost	Comments
Labor	\$23,000	According to Andrew Forster's previous work, using 420 hours of project time and an hourly rate of \$56.25 determines labor costs [6]. The labor costs using the PERT analysis closely relates to Forster's labor costs.
Anticipated Parts	\$39.71	According to Andrew Forster, final bill of material for components resulted in \$39.71 for one PCB board [6]. However, anticipated parts cost could change.
PCB Fabrication	\$92.39	Andrew Forster's previous thesis work calculates PCB Fabrication cost to \$92.39 [6]. However, PCB fabrication could change.

Applying the PERT analysis provides a rough estimate of project duration and labor costs. For labor costs, if assumed \$20,000 for most optimistic, \$23,000 for most likely, and \$26,000 for most pessimistic, then according to equation 1, labor costs estimate at \$23,000. For project duration, if assumed 100 hours as most optimistic, 150 hours for most likely, and 200 hours for most pessimistic, then according to equation 2, project duration estimates at 150 hours. The actual costs incurred were more than anticipated. These are documented below in Table VI:

TABLE VI  
SUMMARY OF ACTUAL PROJECT COSTS

Item	Cost	Comments
Labor	\$23,000	Using 420 hours of project time and an hourly rate of \$56.25 determines labor costs [6]. The labor costs using the PERT analysis closely relates to Forster's labor costs.
Parts	\$306.6	Buying three of each component increased the total amount of parts spent on the project
PCB Fabrication	\$62.65	Buying three PCB's to allow for errors in assembly increased the cost.

The following chapter details the circuit design and simulation process and the challenges encountered. Each iteration shows problems seen and how the situation was remedied.

## Chapter 5: Circuit Design and Simulations

This chapter goes through the circuit design and simulation phase of the project. Simulation through SPICE is the preferred choice for testing circuit designs. The advantages to simulation prototyping is the rapid results of the testing and the very low cost associated with it. The circuit design is built around the LT8390, Linear Technologies 60V Synchronous 4-Switch Buck-Boost Controller, and as a starting point, the test fixture schematic pre-built in the software was used. The .net file used for the simulation can be found in appendix B.

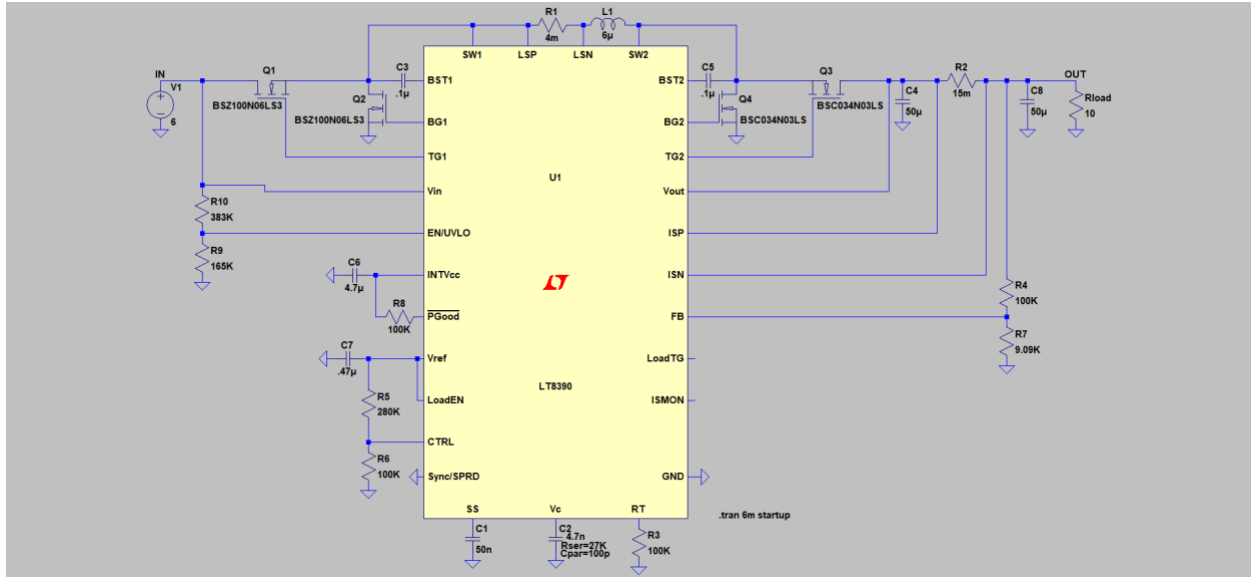


**Figure IV:** LT8390 test fixture schematic.

The following specifications were laid out and used to guide the design:

1.  $V_{in} \in [5,60]$  V
2.  $V_{out} = 36$  V
3.  $I_{outmax} = 7$  A
4.  $\Delta V_{out} = 1$  V
5.  $\eta \geq 90\%$

These goals were derived from the specifications Table I. These specifications, however, were uncertain and shifted upon further iterations. To avoid having to fully simulate multiple inputs, the following corner cases were used:

1.  $V_{in} = 10$  V: *Boost Mode*
2.  $V_{in} = 60$  V: *Buck Mode*
3.  $V_{in} = 37$  V: *Buck Boost Mode*

Using these four test cases, it was assumed that the cases in the middle will follow the same success as the corner cases. Both these test cases were done with two separate loads. One fully resistive load, and the other an electronic load. The starting point for the simulations were provided from Linear Technology's test fixture circuit for the LT8390. Modifications were made to meet our specifications above.

The first goal was to modify the circuit to produce a 36 V output. This was done by altering the feedback resistor network by using equation 1 provided by the datasheet [2]

$$V_{OUT} = 1V \times \frac{R3+R4}{R4} \quad [2] \quad (3)$$

The LT8390 has a voltage feedback pin FB that can be used to program a constant-voltage output, by selecting appropriate values for R3 and R4. In our case, R3 was set to 84.5kΩ, and R4 to 2.4kΩ. Ensuring that the total resistance of the network is large minimizes current flow through the divider network, hence improving efficiency. Selected values are based upon actual resistor values in the market. 0.5% standard resistor values were selected to reduce noise and improve output voltage accuracy.

The switching frequency of the LT8390 is set by an internal oscillator, using a constant frequency control scheme between 150 kHz and 650 kHz. Selection of switching frequency affects efficiency and component size. Low frequency operation improves efficiency by reducing MOSFET switching losses. Since the projects application emphasizes high efficiency and not component sizing, the lowest switching frequency was selected. The switching frequency is set by connecting an appropriate resistor from pin RT to ground. A resistor value of 309 kΩ which corresponds to 150 kHz was used.

The switching frequency and inductor selection are interrelated in that higher switching frequencies allow the use of smaller inductor and capacitor values. Using equation 2 and 3 from the datasheet, the inductor value was properly chosen:

$$L_{buck} > \frac{V_{out} \cdot (V_{inmax} - V_{out})}{f \cdot I_{outmax} \cdot \Delta I_L \% \cdot V_{inmax}} \quad [2] \quad (4)$$

$$L_{boost} > \frac{V_{inmin}^2 \cdot (V_{out} - V_{inmin})}{f \cdot I_{outmax} \cdot \Delta I_L \% \cdot V_{out}^2} \quad [2] \quad (5)$$

Industry recommends selecting  $\Delta I_L \%$  between 0.2 and 0.4 [2]. In this application  $\Delta I_L \%$  was set to 0.3. This value ensures that the converter doesn't operate in discontinuous conduction mode, where the current becomes negative. Equations 2 and 3 provide the critical inductance that meets. Using the specifications above, the inductor value was chosen to be 50 μH, exceeding the critical inductance value. For high efficiency, the inductor must have low core loss, low DC resistance losses, and must handle peak inductor current without saturating.

The LT8390 employs a current mode control for constant frequency operation. In current mode control, an inductor current sense resistor is used to detect and limit the peak inductor current. The sense resistor is chosen based on the required output current. The duty cycle independent maximum current sense thresholds (50 mV in peak-buck and 50 mV in peak-boost) set the maximum inductor peak current in the buck, buck-boost, and boost regions. The sense resistor is calculated using equations 4-7.

$$R_{sense(boost)} = \frac{2 \times 50 \text{ mV} \times V_{in(min)}}{2 \times I_{out(max)} \times V_{out} + \Delta I_L(boost) \times V_{in(min)}} \quad [2] \quad (6)$$

$$R_{sense(buck)} = \frac{2 \times 50 \text{ mV}}{2 \times I_{out(max)} + \Delta I_L(buck)} \quad [2] \quad (7)$$

where,

$$\Delta I_L(boost) = \frac{V_{in(min)} \times (V_{out} - V_{in(min)})}{f_s \times L \times V_{out}} \quad [2] \quad (8)$$

$$\Delta I_L(buck) = \frac{V_{out} \times (V_{in(max)} - V_{out})}{f_s \times L \times V_{in(max)}} \quad [2] \quad (9)$$



The final sense resistor value was chosen to be lower than the calculated sense resistor value in buck and both region, and low equivalent series inductance (ESL). After selecting an appropriate value for the sense resistor, the lowest maximum average load current in boost and buck region can be calculated using equations 8 and 9.

$$I_{out(max\_boost)} = \left( \frac{50 \text{ mV}}{R_{sense}} - \frac{\Delta I_L(boost)}{2} \right) \times \frac{V_{in(min)}}{V_{out}} [2] \quad (10)$$

$$I_{out(max\_buck)} = \left( \frac{50 \text{ mV}}{R_{sense}} - \frac{\Delta I_L(buck)}{2} \right) [2] \quad (11)$$

The LT8390 uses four external n-channel power MOSFETS for the switching scheme. Important parameters for the power MOSFETS include the breakdown voltage  $V_{BR(DSS)}$ , on-resistance  $R_{DS(ON)}$ , reverse transfer capacitance  $C_{RSS}$ , and maximum current  $I_{DS(max)}$ . To select the power MOSFETS, the power dissipated by the MOSFETS must be known. The maximum power dissipation for each switch is calculated using equations 10-13.

$$P_{A(boost)} = \left( \frac{I_{out(max)} \times V_{out}}{V_{in}} \right)^2 \times \rho_T \times R_{DS(ON)} [2] \quad (12)$$

$$P_{B(buck)} = \left( \frac{V_{in} - V_{out}}{V_{in}} \right) \times I_{out(max)}^2 \times \rho_T \times R_{DS(ON)} [2] \quad (13)$$

$$P_{C(boost)} = \left( \frac{(V_{out} - V_{in}) \times V_{out}}{V_{in}^2} \right) \times I_{out(max)}^2 \times \rho_T \times R_{DS(ON)} + k \times V_{out}^3 \times \frac{I_{out(max)}}{V_{in}} \times C_{RSS} \times f_s [2] \quad (14)$$

$$P_{D(boost)} = \frac{V_{out}}{V_{in}} \times I_{out(max)}^2 \times \rho_T \times R_{DS(ON)} [2] \quad (15)$$

The BSZ100N06LS3 G n-channel MOSFET manufactured by Infineon Technologies meets the maximum breakdown voltage  $V_{BR(DSS)}$ , current  $I_{DS(max)}$  and low on-resistance  $R_{DS(ON)}$  which minimizes power losses. Table I shows the absolute maximum ratings of the MOSFETS. Table I shows the maximum breakdown voltage  $V_{BR(DSS)}$  for the four switches during simulation. Switches A and B have a maximum breakdown voltage in the buck region, and switches C and D have a maximum breakdown voltage in the boost region. Table III shows the maximum drain current and drain pulse current for each switch based on simulation. Using simulation, each switch was analyzed for the three cases, determining at what cases the switches deliver maximum drain current and drain pulse current.

Absolute Maximum Ratings	n-channel MOSFET BSZ100N06LS3 G
Breakdown voltage $V_{BR(DSS)}$	60 V
Drain current $I_{DS(max)}$	20 A
Pulse drain current $I_{Dpulse(max)}$	80 A
on-resistance $R_{DS(ON)}$	10 mΩ
Reverse transfer capacitance $C_{RSS}$	24 pF

Table I: Maximum ratings for the n-channel MOSFET BSZ100N06LS3 G from Infineon Technologies [19].

	Switch A	Switch B	Switch C	Switch D
Maximum Voltage Rating	60V	60V	36V	36V

Table II: Maximum voltage ratings for the four external switches based on simulation.

	Switch A	Switch B	Switch C	Switch D
Maximum Drain Current	2.45 A	3.57 A	155.37 mA	6.305 A
Maximum Drain Pulse Current	77.41 A	73.06 A	22.57 A	18.84 A

Table III: Maximum drain and drain pulse current for the four external switches based on simulation. The drain pulse currents last no more than 10 nanoseconds.

The Safe Operating Area graph of the BSZ100N06LS3 G n-channel MOSFET displays the power the MOSFET can handle within a time frame. According to figure V, the MOSFET can handle a maximum pulse power of 4.8 kW for 1 microsecond.

During simulation, all four external switches didn't exceed this power limit,

### 3 Safe operating area

$$I_D = f(V_{DS}); T_C = 25\text{ }^\circ\text{C}; D = 0$$

parameter:  $t_p$

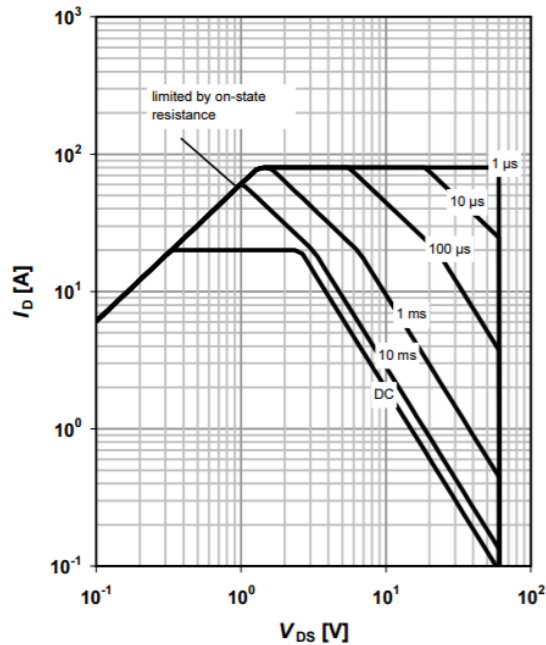


Figure V: Safe Operating Area of the n-channel MOSFET BSZ100N06LS3 G. [19]

The Safe Operating Area shows that the MOSFET has a maximum power dissipation of 4.8 kW, maximum drain to source voltage of 60 V, and maximum permissible drain current of 80 A for a time period of 1 microsecond [19].

Input and output capacitance are necessary to suppress voltage ripple caused by discontinuous current moving in and out of the regulator. 1  $\mu\text{F}$  ceramic capacitors are placed near the regulator's input and output to suppress high frequency switching spikes, and significantly reduce input ripple voltage and power loss.

Input capacitance network is sized to handle maximum RMS current with low equivalent series resistance (ESR). Equation 14 offers a simple worst-case scenario solution commonly used for design, because significant deviations do not offer much relief.

$$I_{rms} = \frac{I_{out(max)}}{2} \quad (16)$$

Output capacitance network is sized to reduce the output voltage ripple and low ESR. The effects of ESR and bulk capacitance must be considered. The output capacitance network is calculated using equations 15 and 16.

$$C_{out(boost)} = \frac{I_{out(max)} \times (V_{out} - V_{in(min)})}{V_{out} \times f_s \times \Delta V_{cap(boost)}} [2] \quad (17)$$

$$C_{out(buck)} = \frac{V_{out} \times (1 - \frac{V_{out}}{V_{in(max)}})}{8 \times L \times f_s^2 \times \Delta V_{cap(buck)}} [2] \quad (18)$$

The final critical output capacitance network is chosen higher than the calculated values in boost and buck region. Choosing a value high ensures that it meets the output voltage ripple specification.

After component sizing of the inductor, sense resistor, MOSFETs, and input and output capacitance network, the three corner cases are simulated using LTSpice. The .net file for the simulations can be found in Appendix B.

#### Corner case 1:

- a)  $V_{in} = 10 \text{ V boost mode}$
- b)  $V_{out} = 36 \text{ V}$
- c) electronic load = 0.277 A
- d) resistive load = 130  $\Omega$

For corner case 1, the input voltage is set to 10 V with two different loads: a current source which acts as an electronic load, and a resistive load. Simulation of two different loads ensures that the circuit doesn't alter the user experience of the elliptical machine. The electronic load is based on assuming 100% efficiency. At 10 V, the elliptical machine produces 1 A, and thus 10 W. Using the power equation  $P = V_o \times I_o$  and an output voltage of 36 V, an  $I_o$  of 0.277 A is calculated and used to validate the corner case works. Using the power equation  $P = \frac{V^2}{R}$  and an output voltage of 36 V, a resistive load of 130  $\Omega$  is calculated and used to validate the corner case works. At low load of 10 W, the efficiency decrements, with an efficiency of 54.4%.

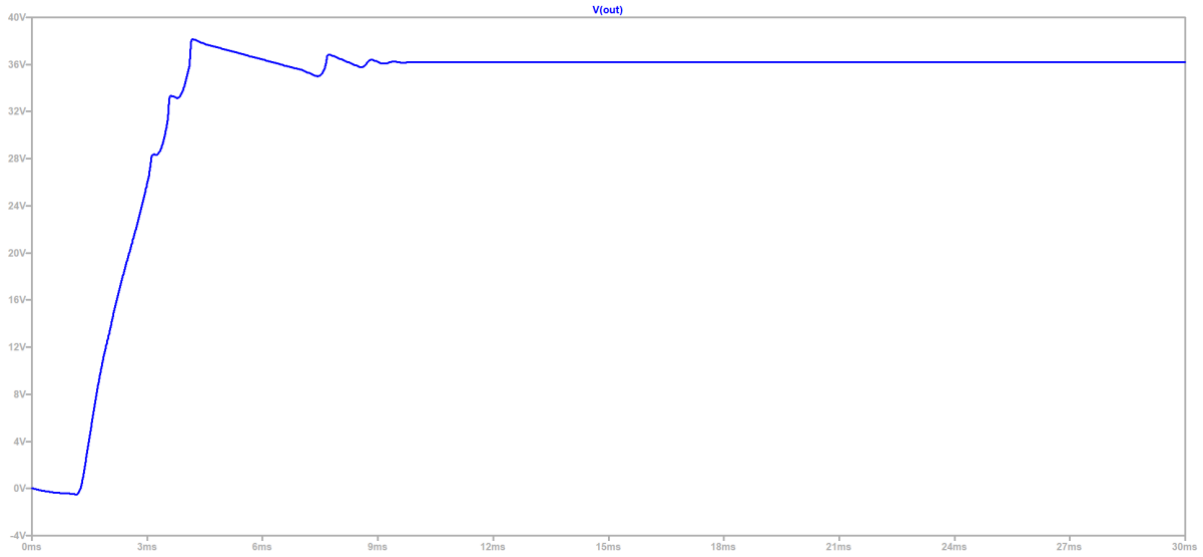


**Figure VI:** 36 V output voltage and less than 1 V output voltage ripple with 0.277 An electronic load.

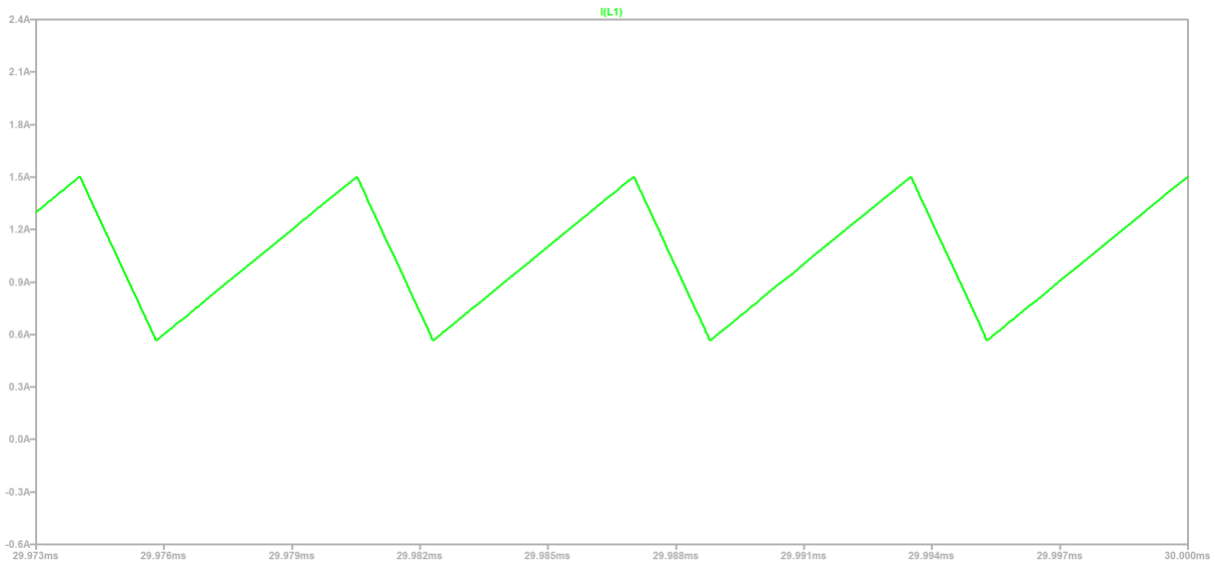


**Figure VII:** Boost region inductor current waveform using electronic load.

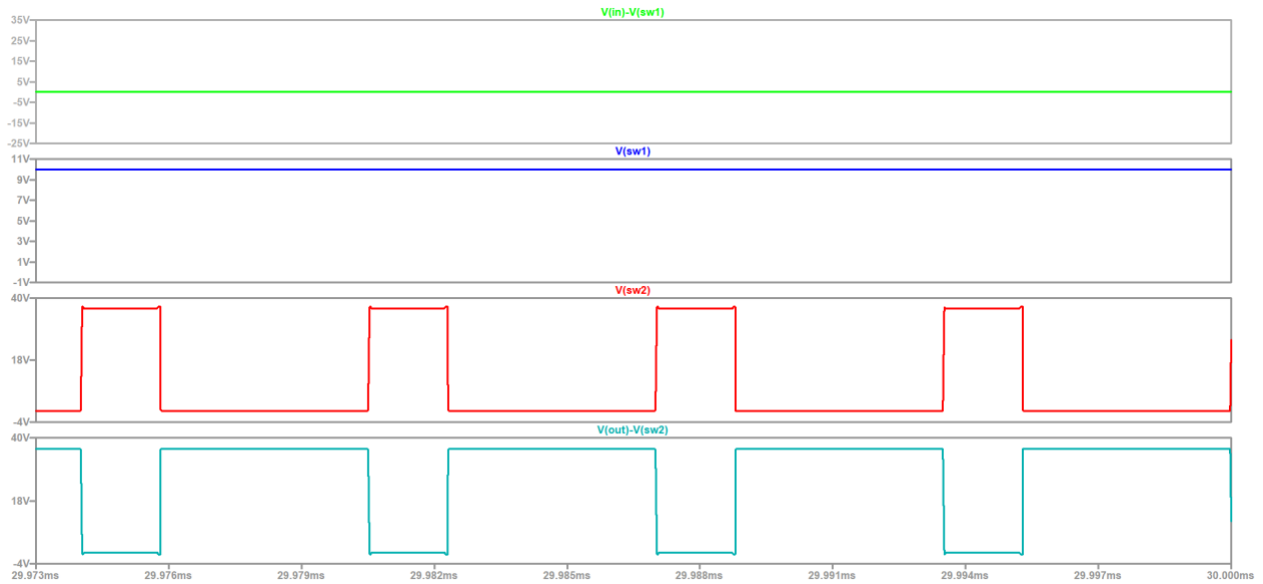


**Figure VIII:** Drain to Source voltage waveforms for four external MOSFET switches using electronic load. As expected in boost region, switches C and D alternate, switch A is always on, and switch B is always off.

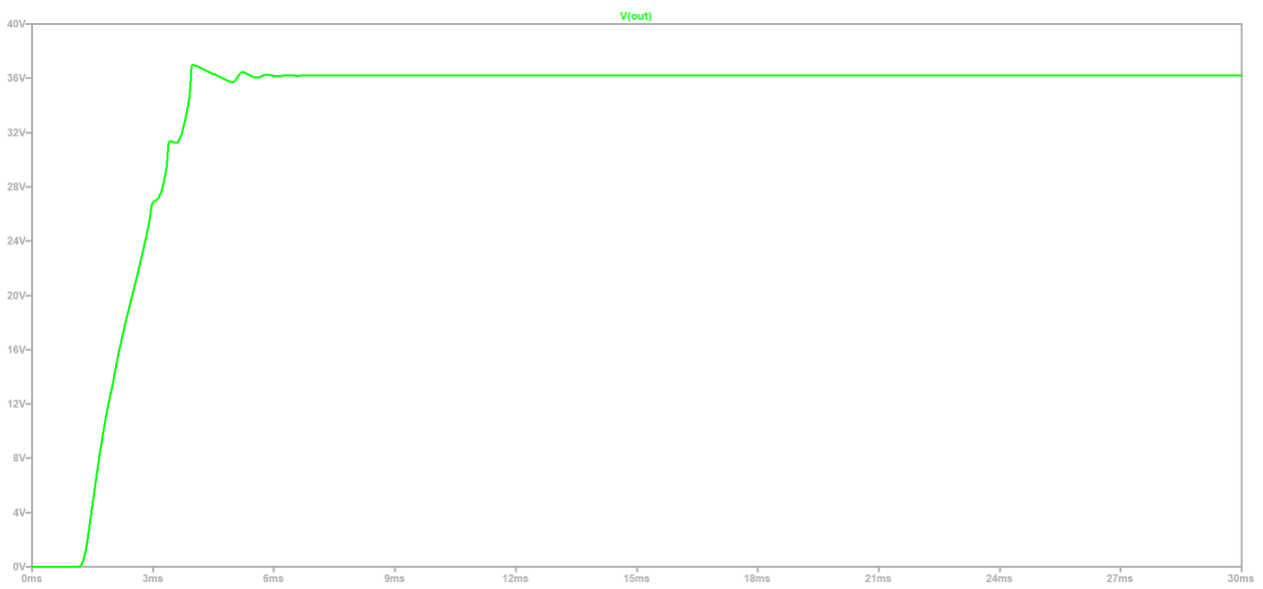


**Figure IX:** 36 V output voltage and less than 1 V output voltage ripple with 130  $\Omega$  resistive load.

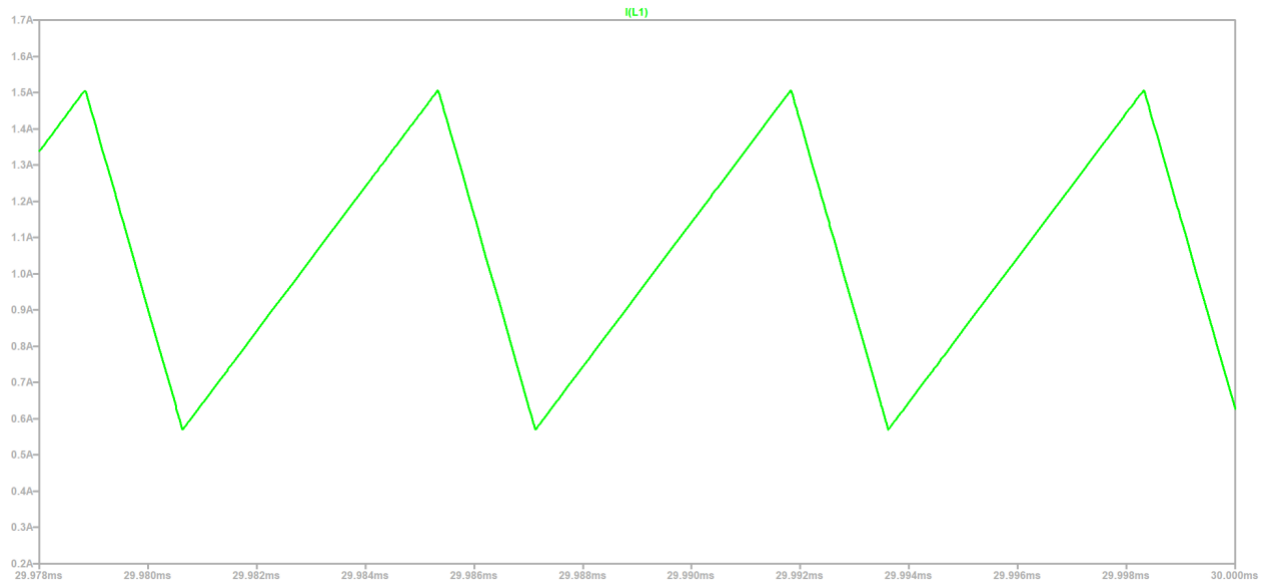


**Figure X:** Boost region inductor current waveform using a resistive load.

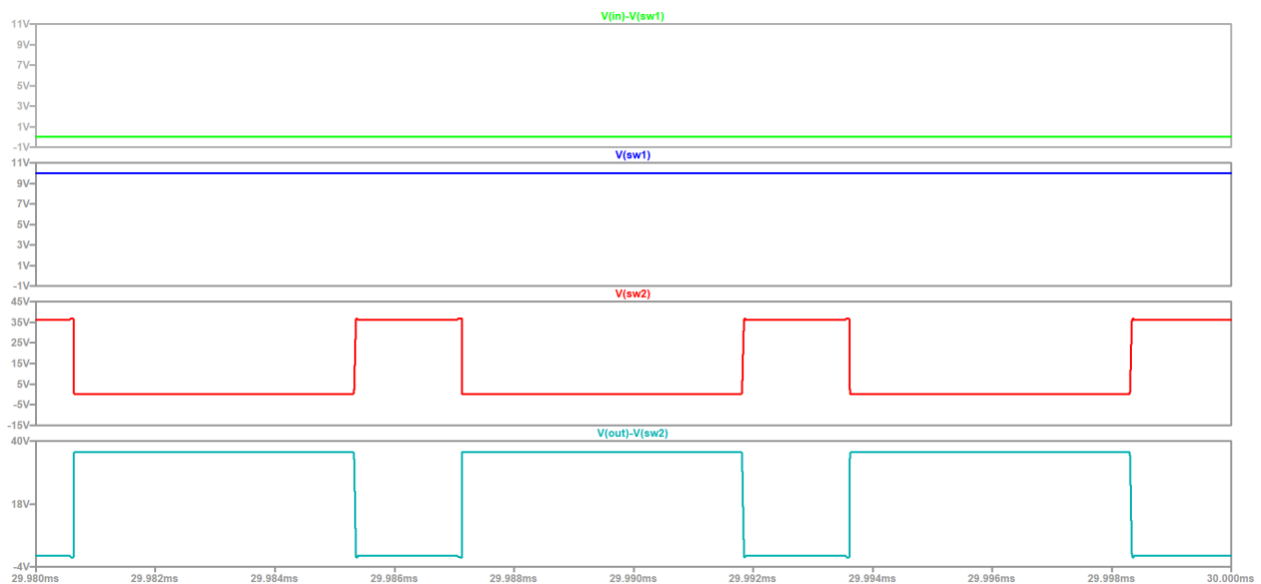


**Figure XI:** Drain to Source voltage waveforms for four external MOSFET switches using a resistive load. As expected in the boost region, switches C and D alternate, switch A is always on, and switch B is always off.

**Corner case 2:**

- a)  $V_{in} = 60\text{ V}$  buck mode
- b)  $V_{out} = 36\text{ V}$
- c) electronic load = 5.4 A
- d) resistive load = 5.3  $\Omega$

For corner case 2, the input voltage is set to 60 V with two different loads: a current source which acts as an electronic load, and a resistive load. Simulation of two different loads ensures that the circuit doesn't alter the user experience of the elliptical machine. The electronic load is based on assuming 100% efficiency. At 60 V, the

elliptical machine produces 6 A. The current source acting as an electronic load is calculated using  $P = I_o \times V_o$ . At 100 % efficiency, the elliptical machine delivers 360 W. Using a power of 360 W and  $V_o$  of 36 V, a current source of 10 A is calculated. However, after several simulation attempts, 5.4 A is the maximum current load the controller provides. Using  $P = \frac{V_o^2}{R}$ , P of 360 W, and  $V_o$  of 36 V, a resistive load of 3.6  $\Omega$  is calculated. However, after several simulation attempts, the minimum resistive load the controller works with is 5.3  $\Omega$ . At high loads, the efficiency increases to 92.9%.

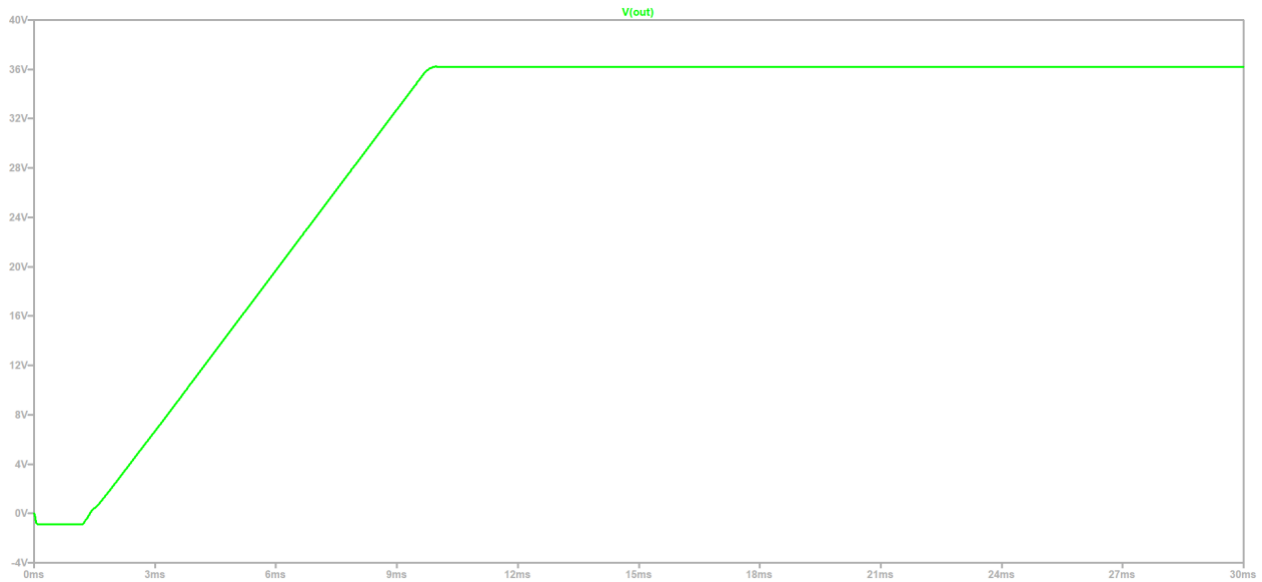


**Figure XII:** 36 V output voltage and less than 1 V output voltage ripple with 5.4 An electronic load.

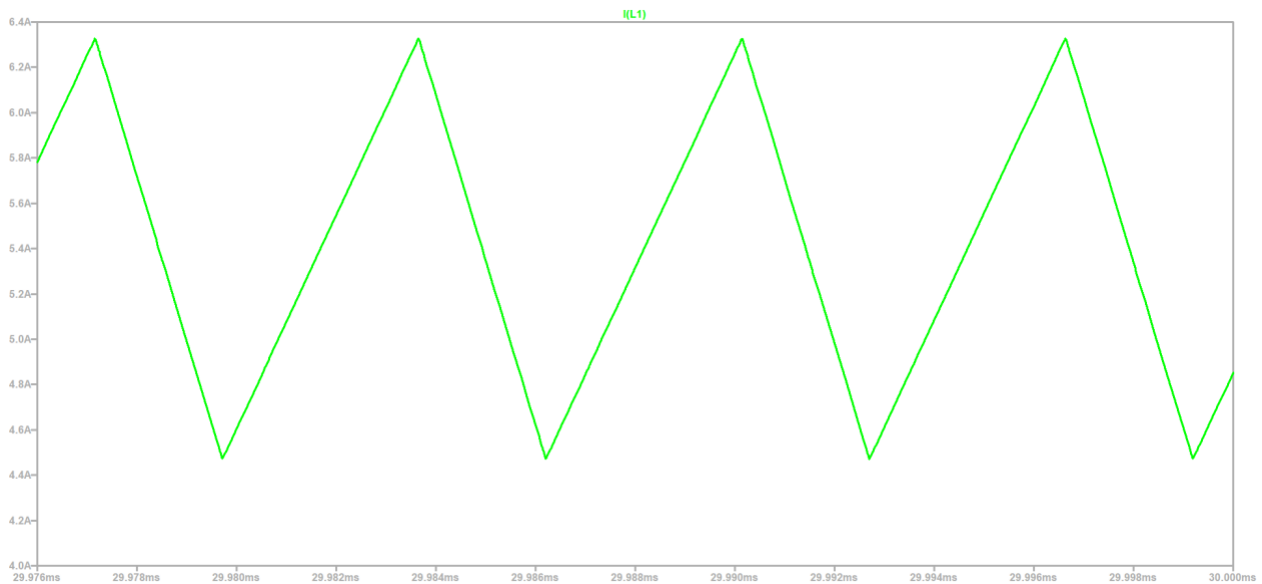


**Figure XIII:** Buck region inductor current waveform using electronic load.

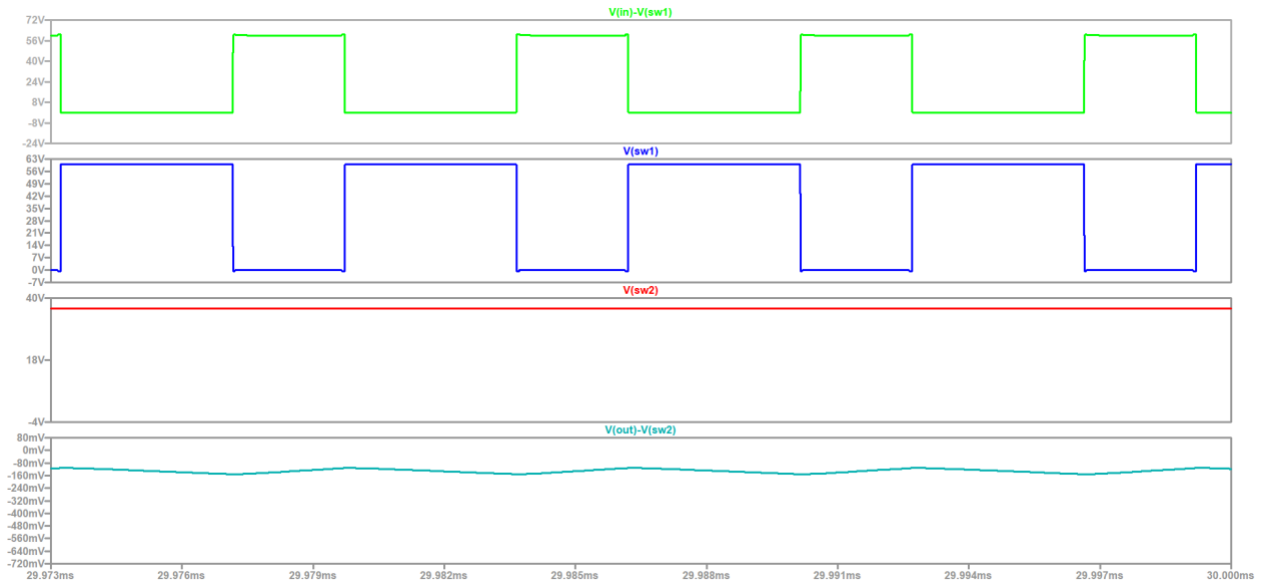


**Figure XIV:** Drain to Source voltage waveforms for the four external MOSFET switches using an electronic load. As expected in the buck region, switches A and B alternate, switch D is always on, and switch C is always off.

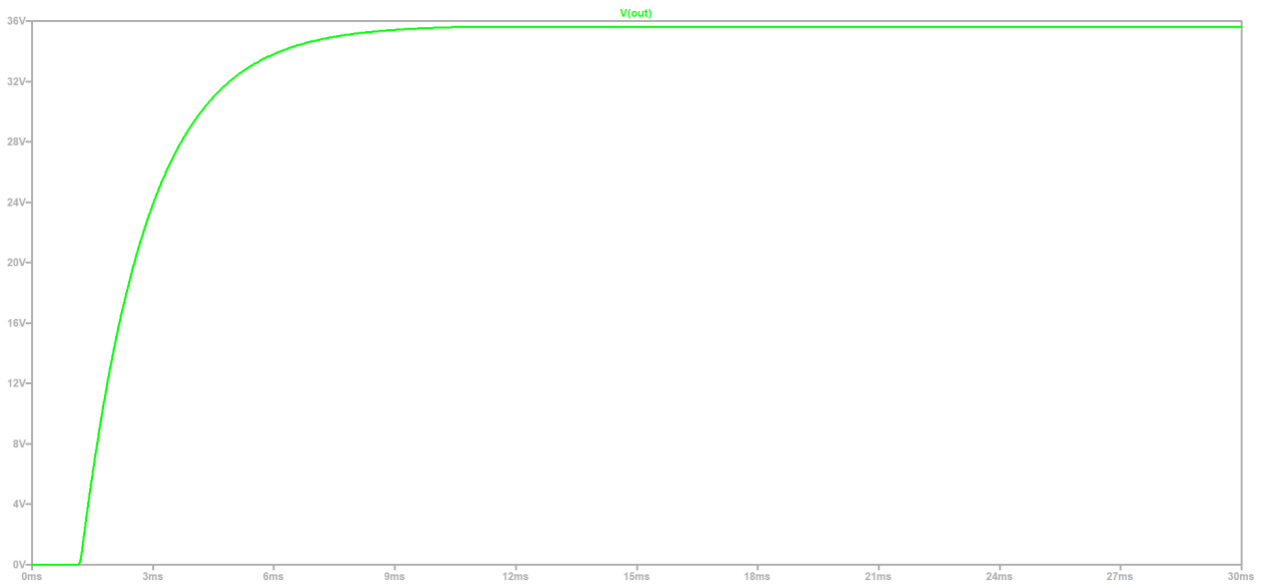


**Figure XV:** 35.61 V output voltage and less than 1 V output voltage ripple with 5.3  $\Omega$  resistive load.



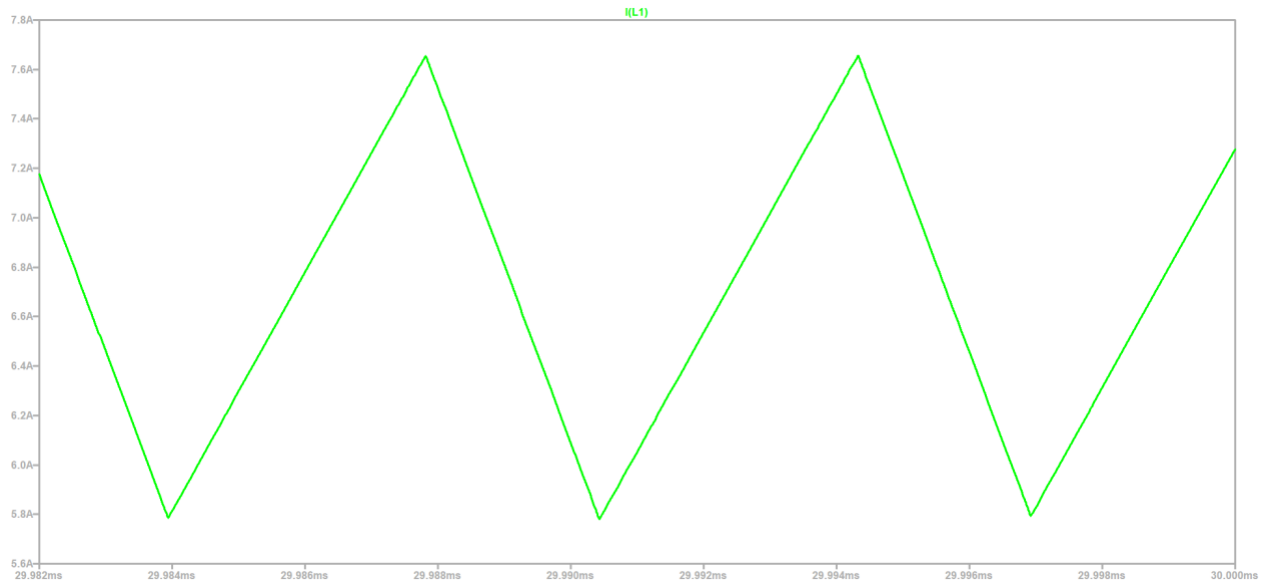


**Figure XVI:** Buck region inductor current waveform using a resistive load.

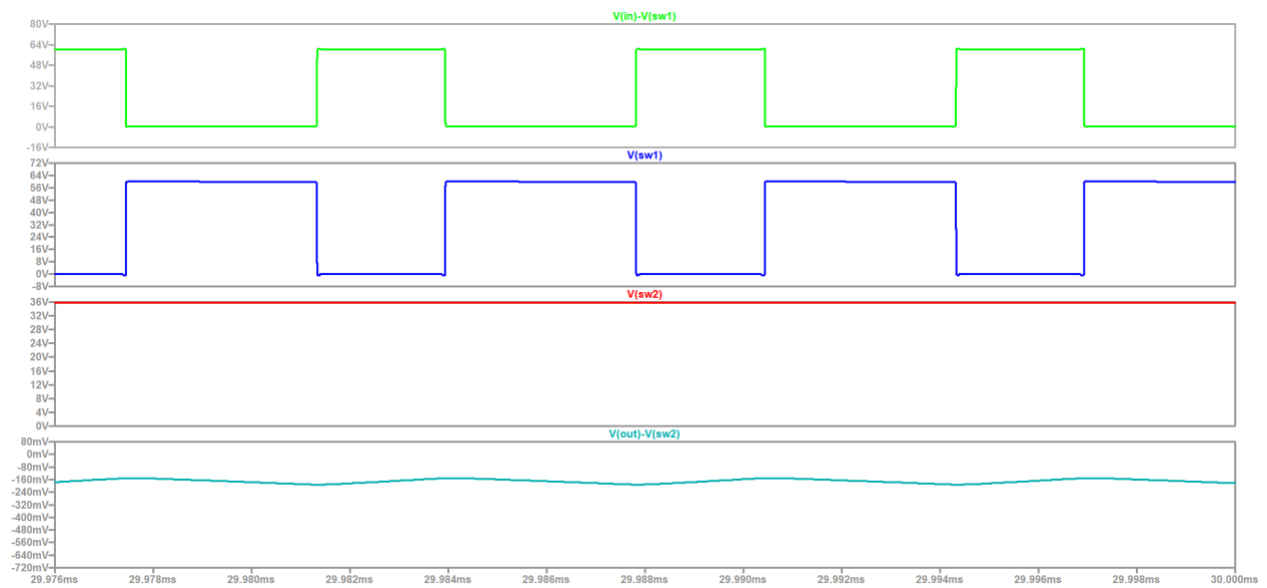


**Figure XVII:** Drain to Source voltage waveforms for the four external MOSFET switches using a resistive load. As expected in the buck region, switches A and B alternate, switch D is always on, and switch C is always off.

### Corner case 3:

- a)  $V_{in} = 37\text{ V}$  buck boost mode
- b)  $V_{out} = 36\text{ V}$
- c) electronic load = 3.7 A
- d) resistive load =  $10\ \Omega$

For corner case 3, the input voltage is set to 37 V with two different loads: a current source which acts as an electronic load, and a resistive load. Simulation of two different loads ensures that the circuit doesn't alter the user experience of the elliptical machine. The electronic load is assuming a current-voltage linear relationship. At 10 V the elliptical machine produces 1 A, and at 60 V the elliptical machine produces 6 A, therefore, for an input voltage of 37 V, it is assumed the elliptical machine produces 3.7 A. Efficiency is assumed 100%. Using the power equation  $P = \frac{V^2}{R}$ , P of 137 W, and an output voltage of 36 V, a resistive load of  $10\ \Omega$  calculated. Efficiency slightly decreased to 91.9%.



**Figure XVIII:** 36.19 V output voltage and less than 1 V output voltage ripple with 3.7 An electronic load.



**Figure XIX:** Buck-boost region inductor current waveform using an electronic load.

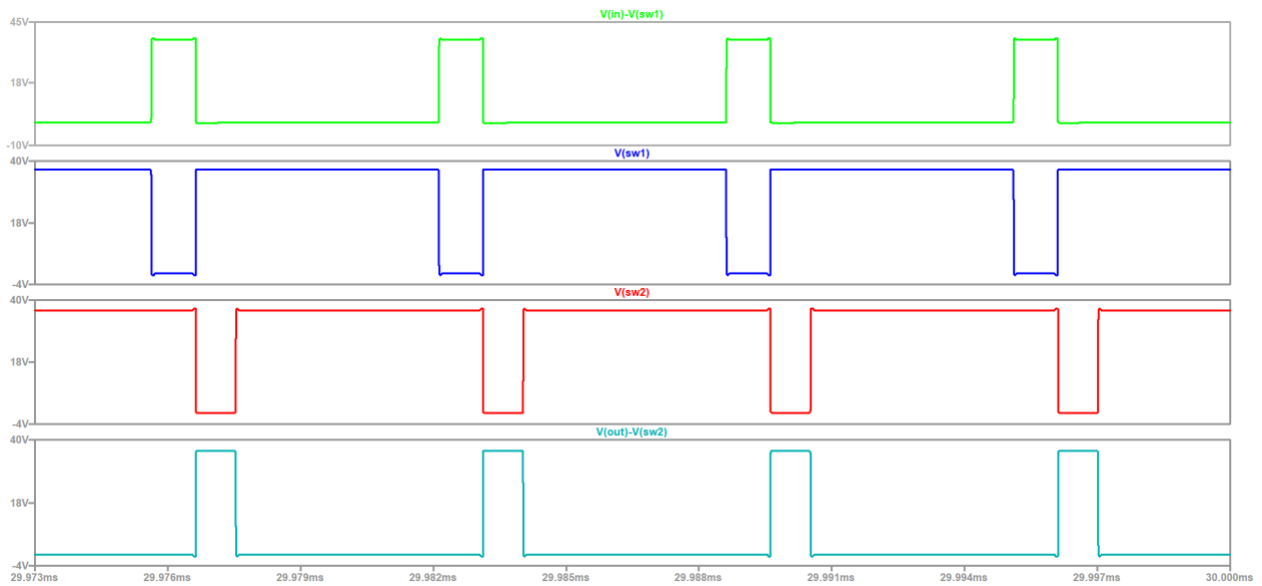


**Figure XX:** Drain to Source voltage waveforms for the four external MOSFET switches using an electronic load. As expected in the buck-boost region, all switches alternate at different duty cycles. Switch C has a duty cycle of approximately 15% and switch D has a duty cycle of approximately 85%.

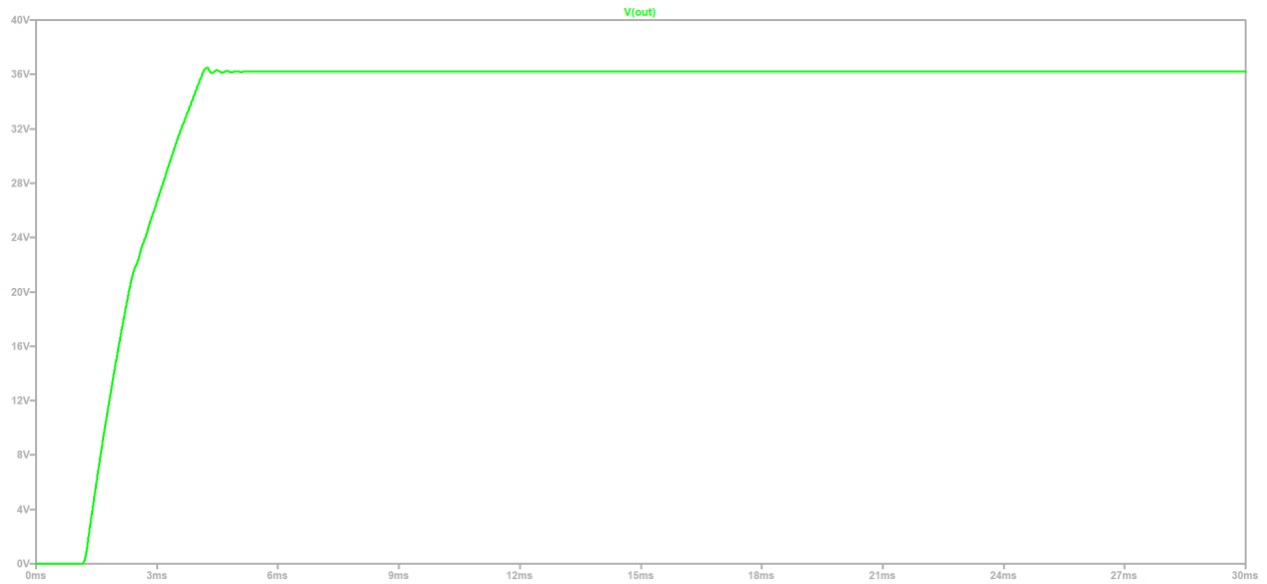


**Figure XXI:** 36.19 V output voltage and less than 1 V output voltage ripple with 10  $\Omega$  resistive load.

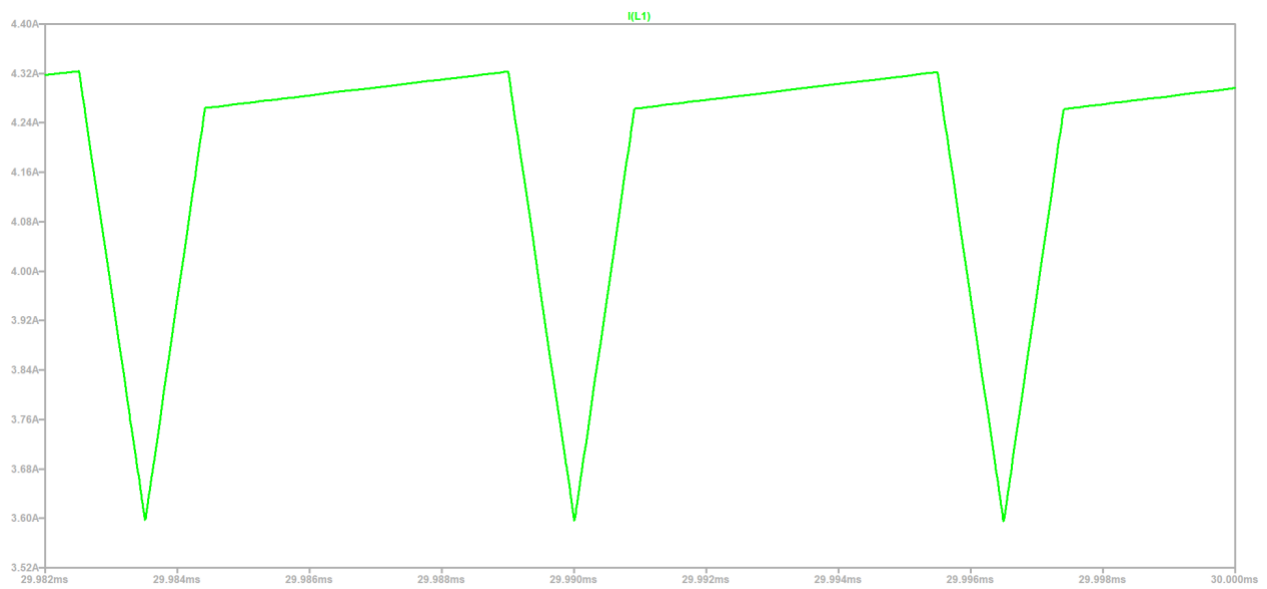


**Figure XXII:** Buck-boost region inductor current waveform using a resistive load.

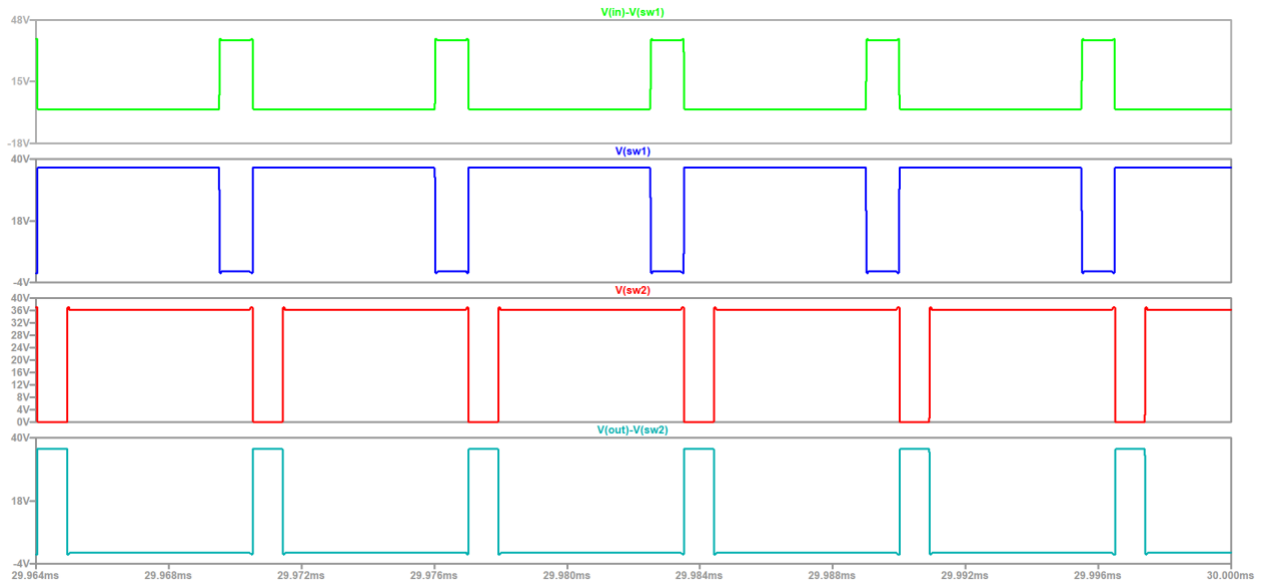


**Figure XXIII:** Drain to Source voltage waveforms for the four external MOSFET switches using a resistive load. As expected in the buck-boost region, all switches alternate at different duty cycles. Switch C has a duty cycle of approximately 15% and switch D has a duty cycle of approximately 85%.

After successful simulations for the corner cases and rigorous component sizing calculations, the next step is the PCB layout consideration. The next chapter documents the PCB layout design, including component layout choices, and struggles faced during the process.

## Chapter 6: Component Selection and PCB Layout

This section walks through the selection of the components and the criterion it was based upon. Following the component selection, the process of laying out the board is documented along with the design considerations. The board design and layout are done using KiCad. KiCad is being because it is free, open-source, and easy to use.

The first components selected were the power MOSFETs necessary for providing the switching capabilities. Due to the input voltage range varying from 5-60 volts, the input MOSFETS need a  $V_{DS}$  breakdown voltage of at least 60 V. With the output voltage at a constant 36 V, the output MOSFETS need a  $V_{DS}$  breakdown voltage of at least 36 V. The max current seen is 8 A, so the MOSFETS need to be able to handle this. The component values need to include a safety margin if a circuit failure occurs. The Infineon power series BSZ100N06LS3 NMOSFET provided a great solution and met the specifications required. This MOSFET was provided in the LTSpice test bench for the LT 8390 and no other MOSFETs were considered because these fully met the specifications. Table VI shows the necessary specifications for the NMOSFET.

Table VI  
BSZ100N06LS3 NMOS Specifications [19]

Specification	BSZ100N06LS3
$V_{DS}$ Breakdown Voltage	60 V
Current Rating	20 A
$R_{DS}$ On	10 m $\Omega$
Input Capacitance	2.6 nF
Max Power Dissipation	50 W

In order for the microinverter to efficiently handle the output voltage of the converter, the output voltage ripple must be reduced to a minimum. The specifications in table I define an output voltage ripple of 1.8 volts. After the first iteration, seen in figure V, the output ripple extremely exceeded this value. To reduce this, a large 620  $\mu$ F capacitor was introduced to the output voltage node. This value was arbitrarily chosen as a starting point to tweak the output capacitance. This largely decreased the output ripple seen in the simulations. One concern was the total equivalent series resistance of the capacitors. If the ESR were to be too high, it causes high losses in the capacitor along with additional unwanted ripple. Upon learning the efficiency of the converter was lower than anticipated, about 84%, the output capacitance is reduced. This could be done because the output ripple specification had some room to change. The efficiency of the converter rose to meet our specification, about 96%.

Other design considerations to keep in mind were the package footprint, frequency ratings, cost, and availability, but these design considerations required less thought as those mentioned above. Figure XXIV shows the schematic for the first revision. Table V shows the preliminary estimate for costs.

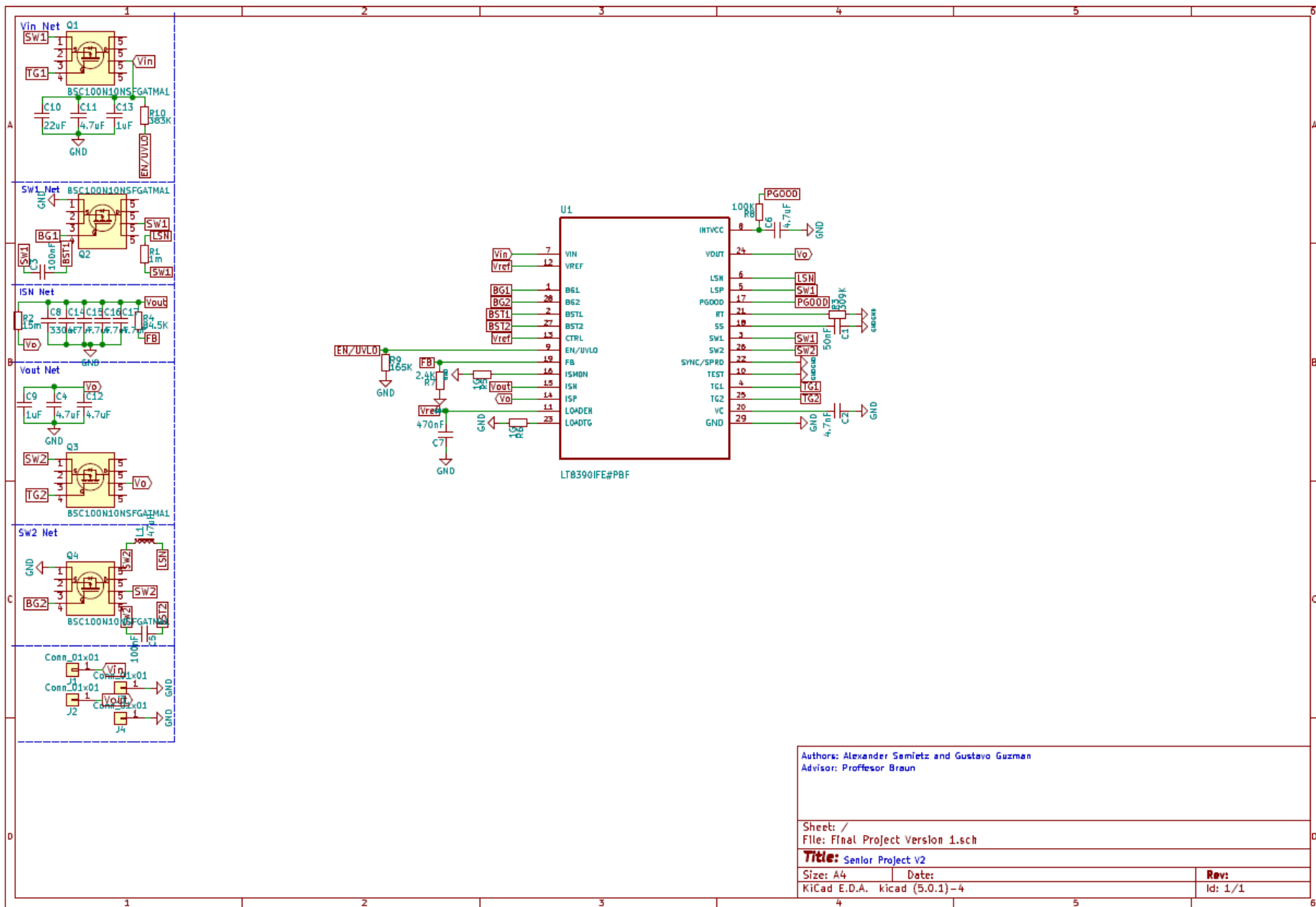


Figure XXIV: Schematic for First Revision of Board

The LT8390 datasheet provides valuable information and important considerations for laying out the PCB. Some of the more notable examples include, placing switch A and the input capacitance, and switch B and the output capacitance as close to the IC as possible, placing the negative terminals of the capacitors as close as possible, and using planes for  $V_{in}$  and  $V_{out}$ . To manufacture the PCB, expressPCB and their MiniBoardPlus Service is used. This service sets out certain footprint of 3.8 x 2.5 inches which puts constraints on the number of components and the real estate to layout the components on the board. The first revision of the board is seen in figures XXV and XXVI.

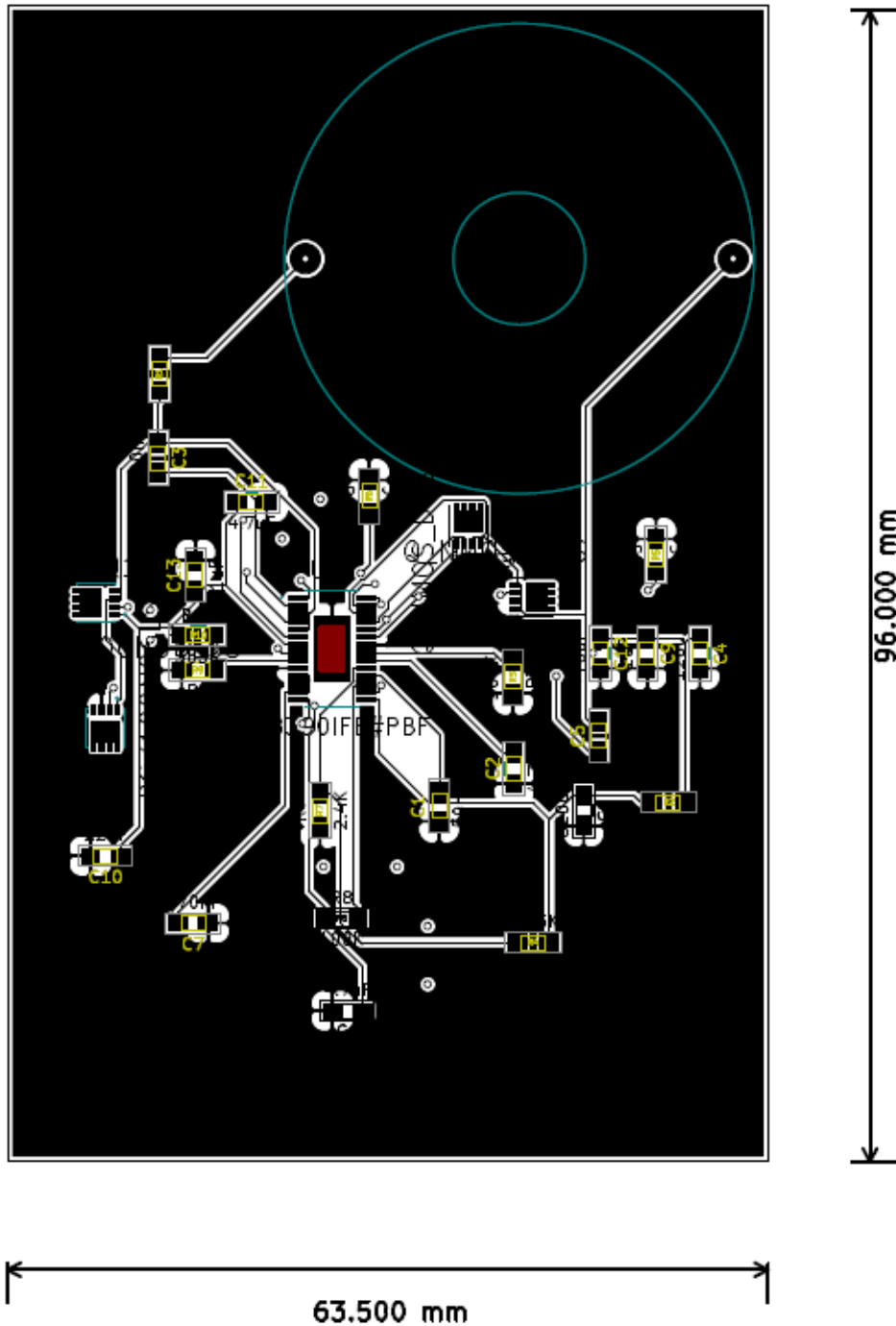


Figure XXV: Front Layer for First Revision of Board



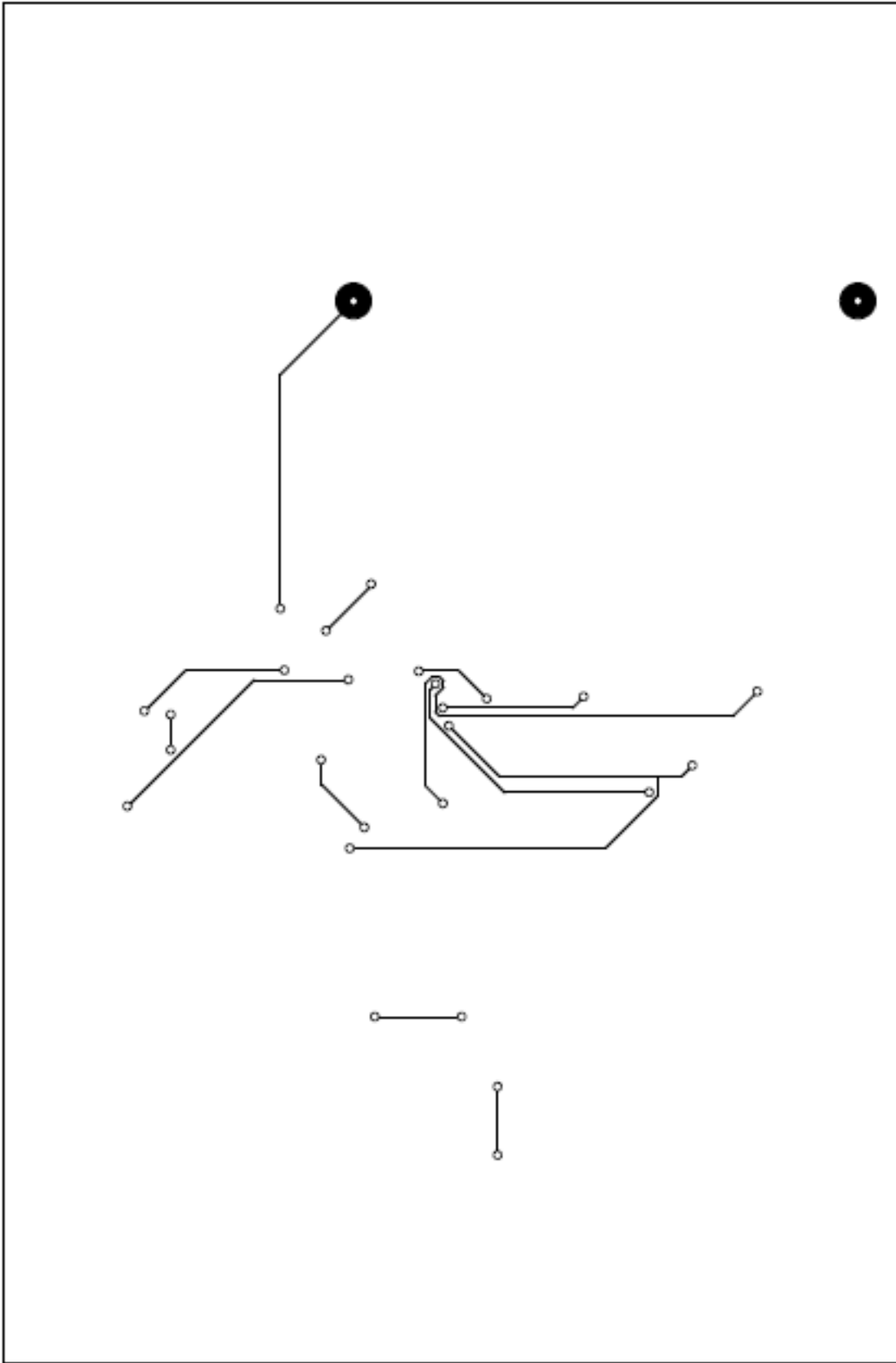


Figure XXVI: Back Layer for First Revision of Board

Some struggles first encountered when laying out this board were the large amount of considerations to keep in mind. Keeping the board organized while also trying to pay attention to important nuances took a large amount of time. Once all the components were in a reasonable configuration it was time to route all the nets to their connections. Thanks to auto-routing tool, the traces were made. Once the auto-routing tool was completed, a couple modifications had to be made. The first modification was the minimum trace width needed for the ground plane. The minimum trace width was too large which didn't allow the GND pin, which was near the other pins, to be connected to the ground pour. The minimum trace width was reduced which remedied the issue. The other modification needed was due to some isolated ground pours not connecting on the front layer. Vias were used to connect these ground pours together. Other slight changes were made, such as small route changes and small components movements to give more room for the traces.

Upon reviewing the first revision, multiple aspects on the board required attention. First, the board had no access to reach the outside world. Three, four millimeter, holes are added allowing banana plug terminals to be screwed through the board. One for Vin, Vout, and GND. Many of the components also had no way of dissipating heat, so the critical power components had several thermal vias added. Finally, the power lines were given wider trace widths to permit the high current seen in the switching modes of the converter. These changes are seen in figures XXVII through XXIX.

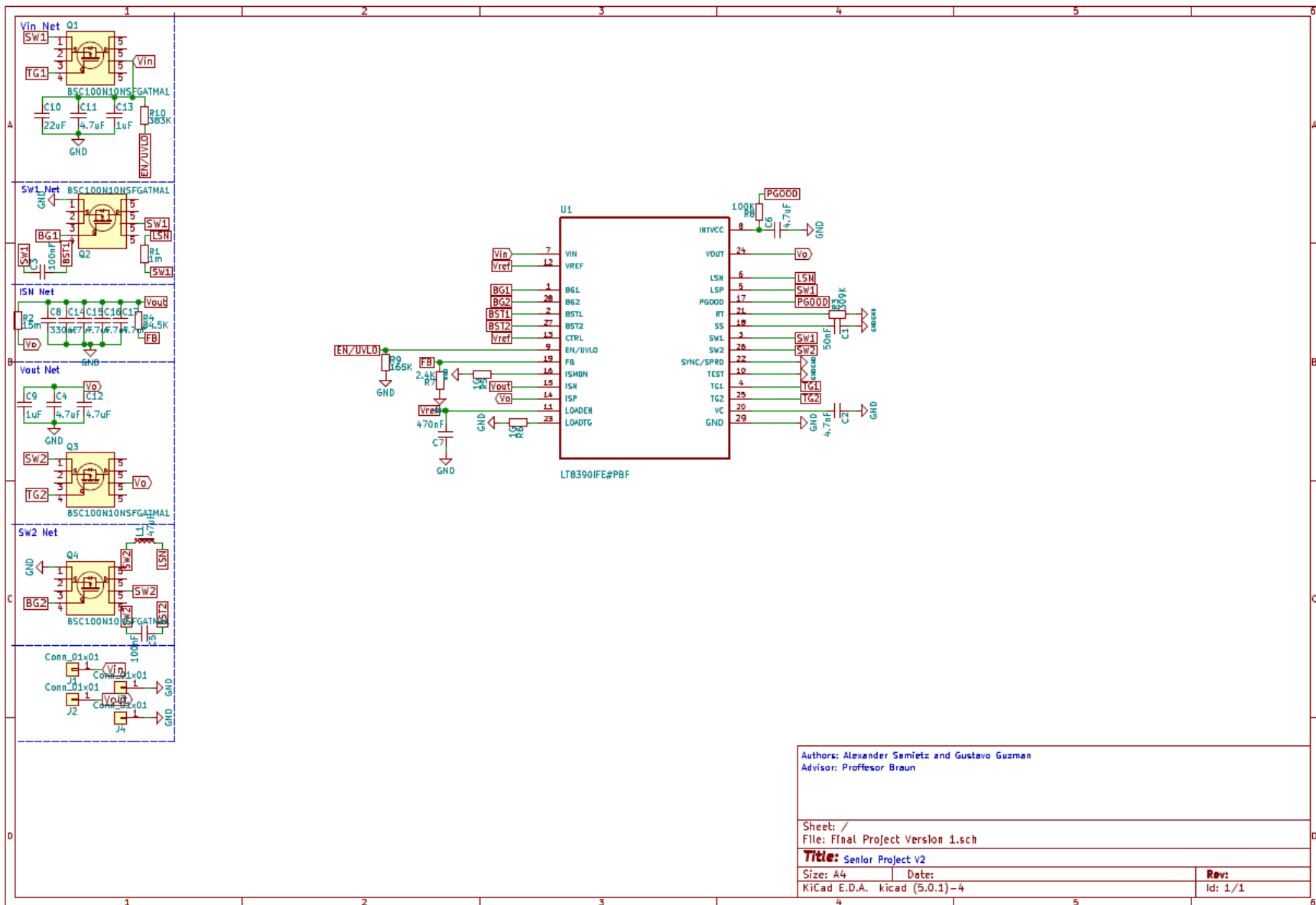


Figure XXVII: Schematic for Second Revision of Board

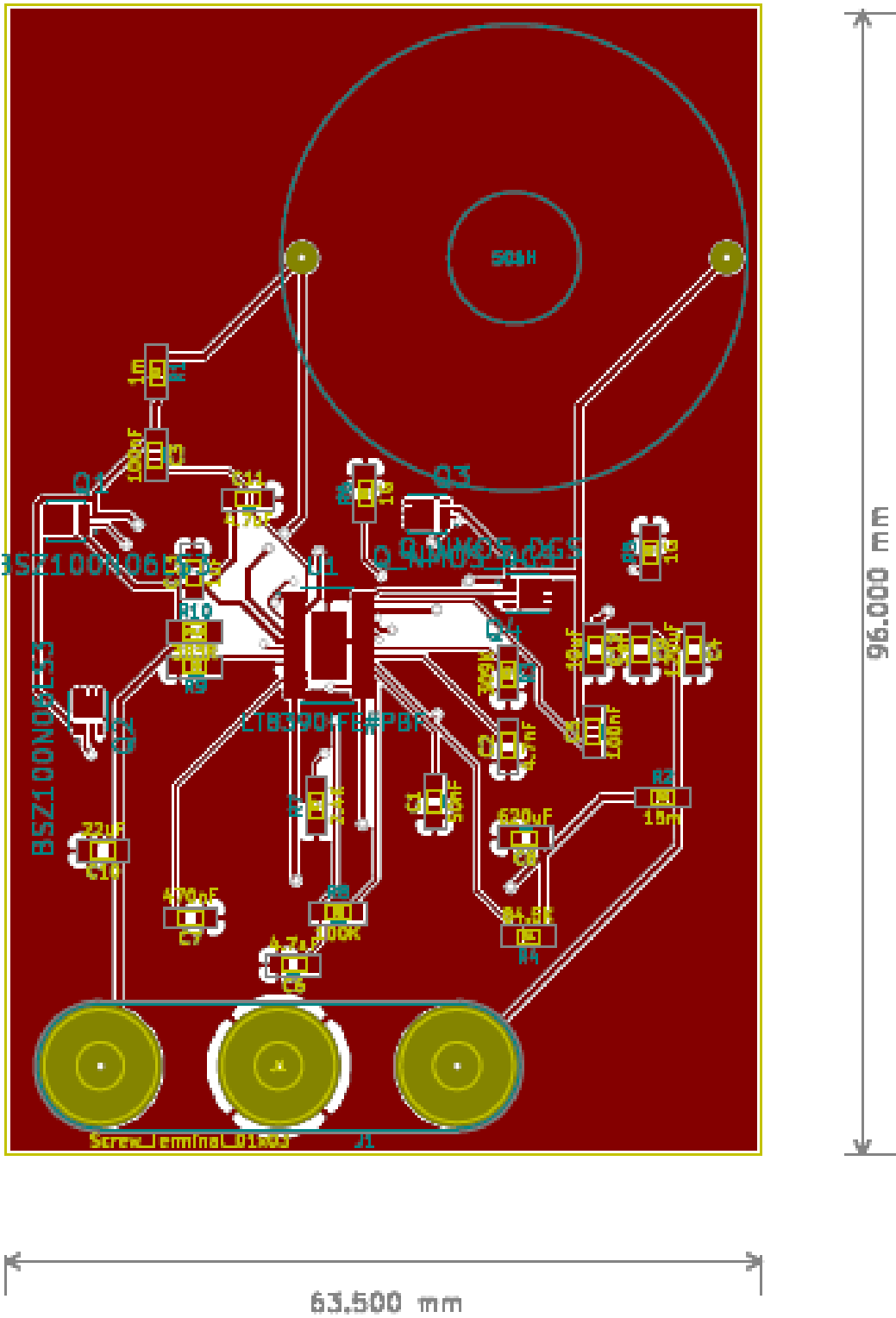
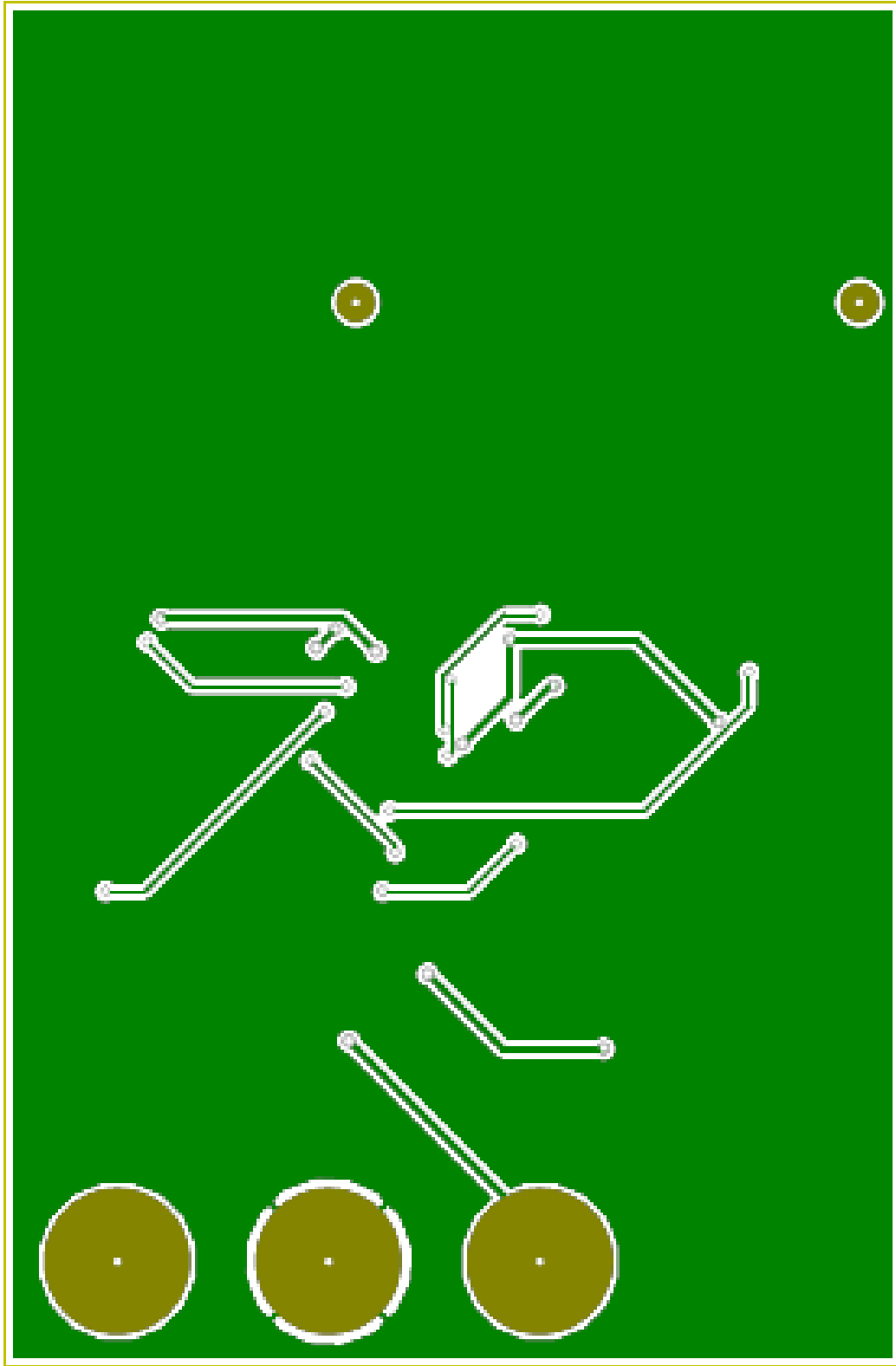
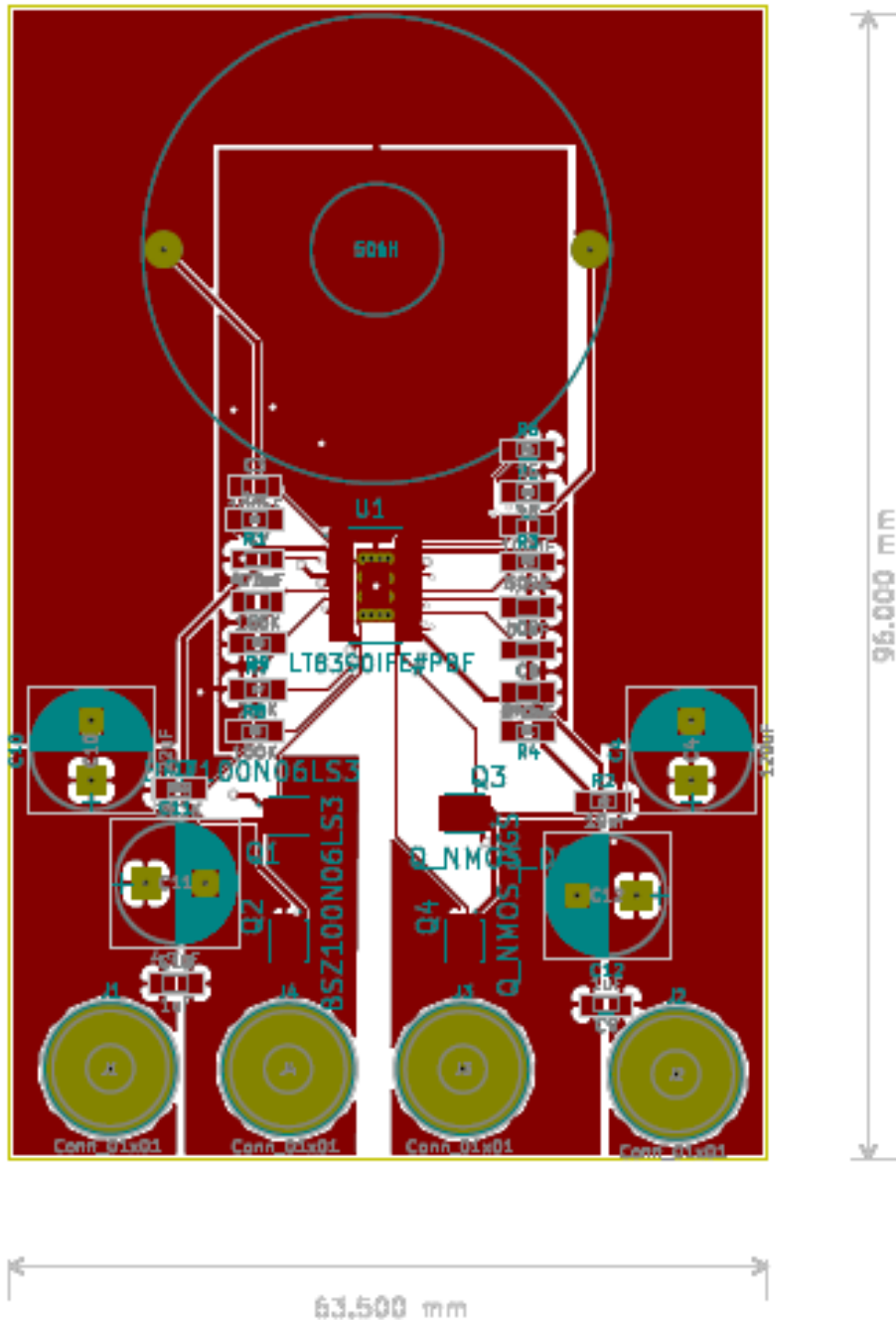


Figure XXVIII: Front Layer for Second Revision of Board



**Figure XXIV:** Back Layer for Second Revision of Board

After discussions with Professor Braun and reviewing the second revision of the board, several major issues were found. The main issue with both revisions of the board was the lack of power planes for many of the nets. The traces defined for the power paths would not handle the high current. Power planes were added for the Vin, SW1, LSN, SW2, Vo, and Vout nets to handle the large amount of current, and thus power. The power path follows the direction seen by the black arrows in figure XXXIV. The digital signals, which produce far lower currents, are found in the middle of the board closest to the IC. Two separate ground planes were created allowing the signals to return to the correct plane from which it was originated. Thermal vias were added to the bottom of the IC to prevent overheating. Vin and Vout both needed separate ground plugs, so another plug was added. No new components were added, so refer to figure XXVIII for schematic.



**Figure XXXI:** Front Layer for Third Revision of Board

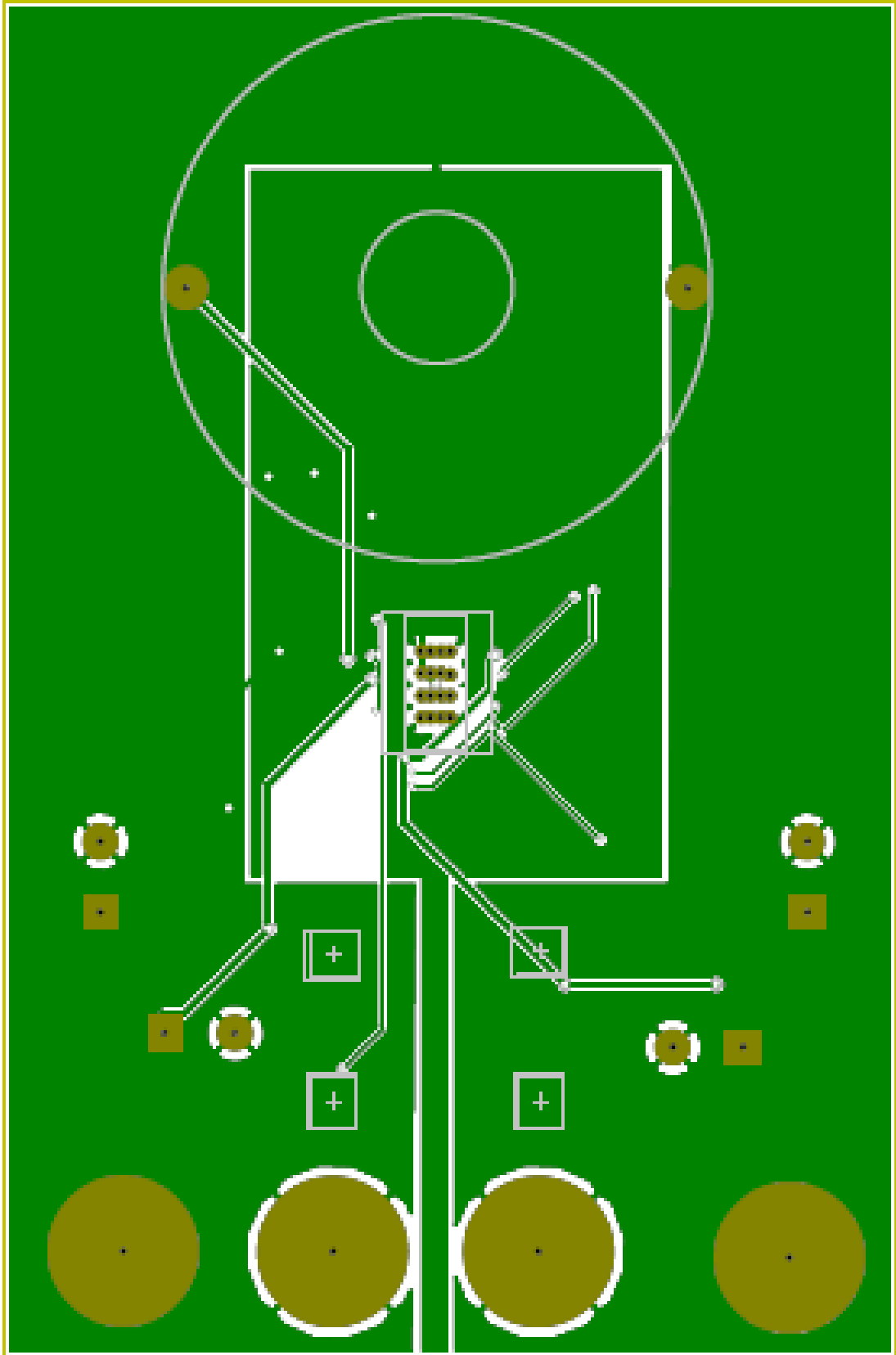


Figure XXXII: Back Layer for Third Revision of Board

Small, quality-of-life, changes were made to the third revision to complete the board. The digital plane was shrunk to shorten the return path for digital signals. A new inductor was switched out for the previous chosen one, so a new footprint was created to accommodate this change. Paths that had originally thought to handle low currents were increased due to their actually high current loads. Finally, test points were added to the gates of each transistor and on opposite sides of the sense resistors for troubleshooting purposes.



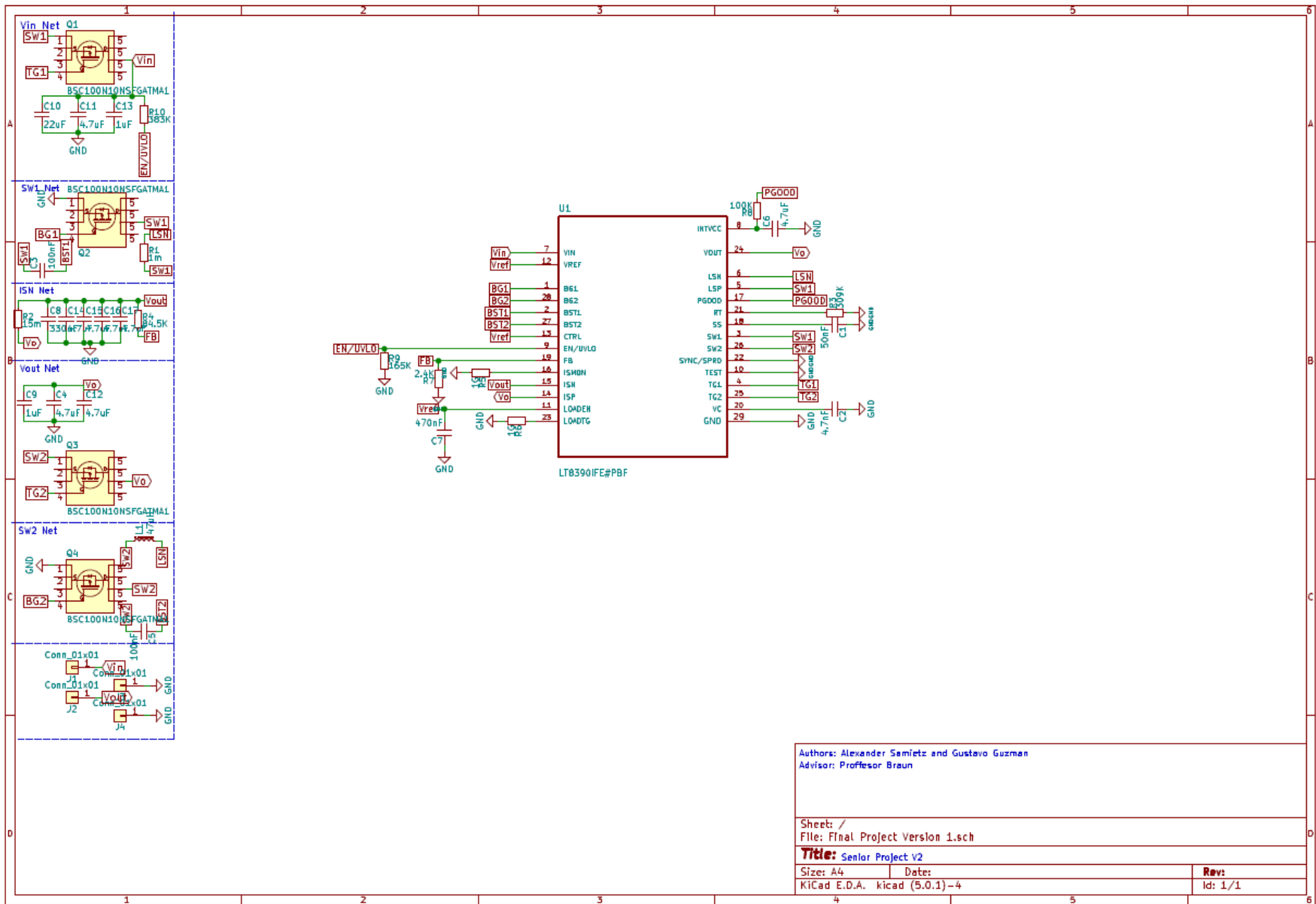


Figure XXXIII: Schematic for Final Revision of Board

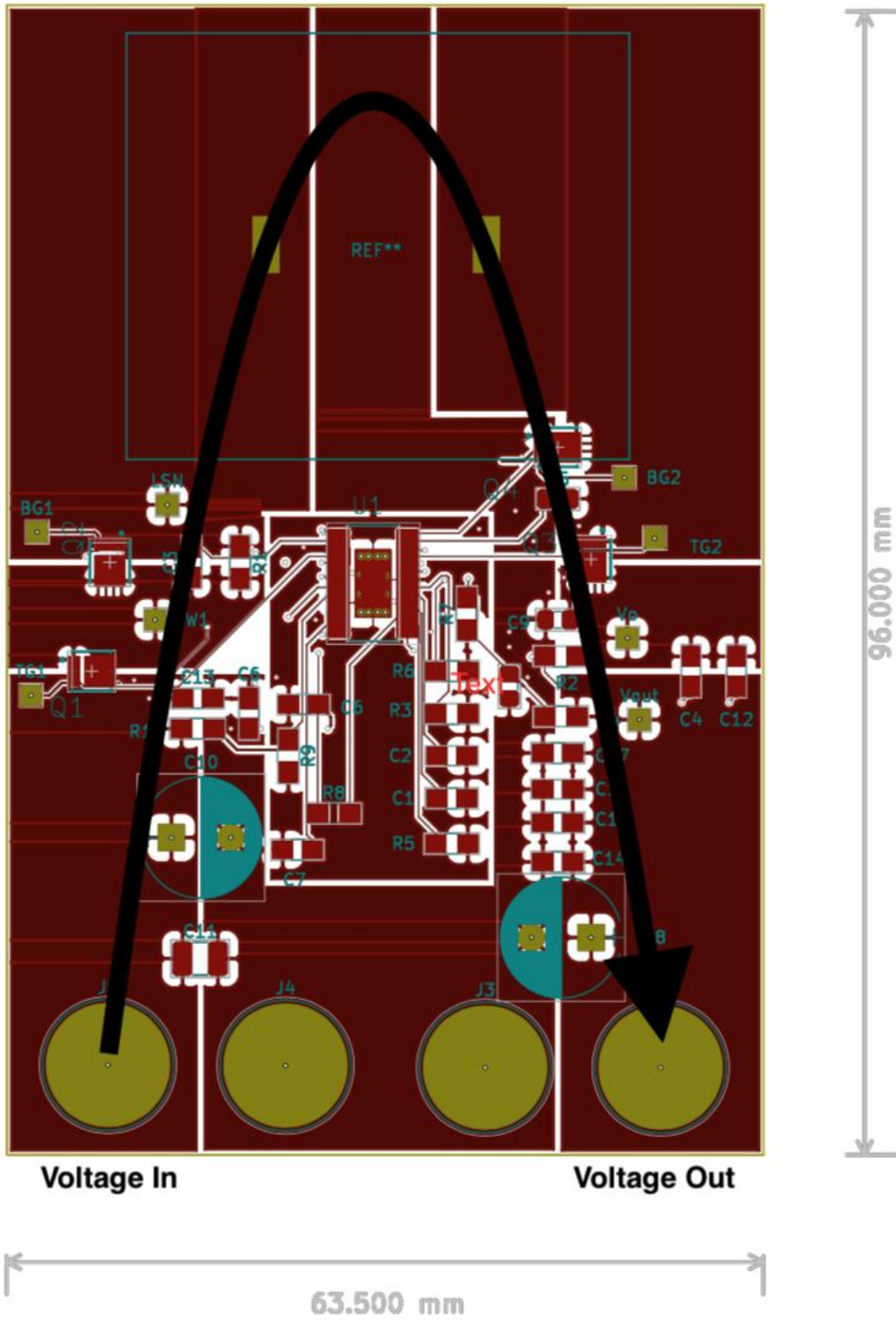
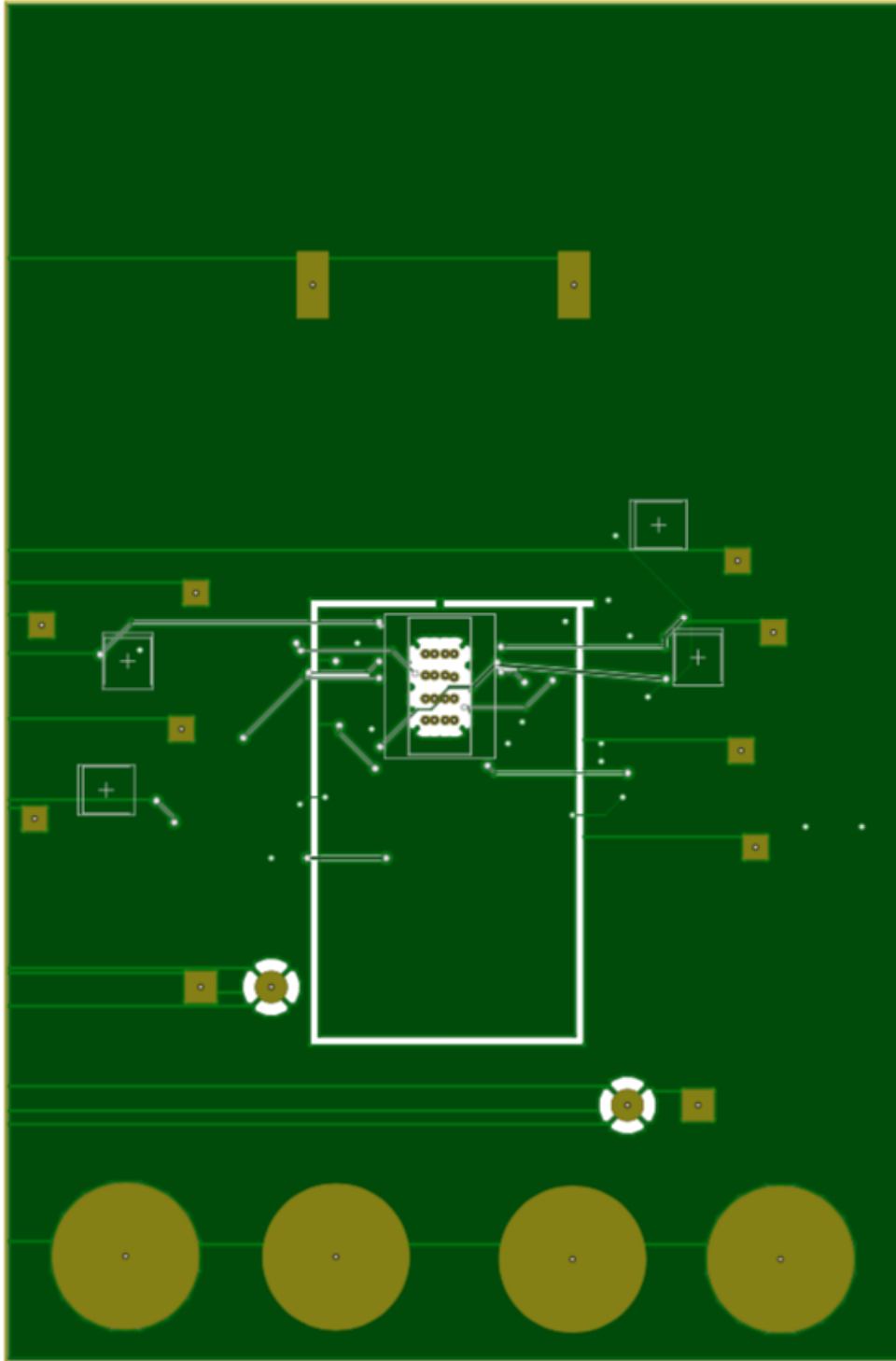


Figure XXXIV: Front Layer for Final Revision of Board



**Figure XXXV:** Back Layer for Third Revision of Board

OSH Park was used as the fab house for this design. They provide an easy to use interface for uploading designs and cost-effective boards. The next chapter outlines the assembly of the PCB's and the issues faced during this process.

## Chapter 7: Assembly

After receiving the PCB's from OSH Park, the assembly process started. The lack of a solder stencil required hand soldering for all the components. This required precise soldering for the IC and the MOSFETs. Using the Hakko FX-888D the soldering portion of the process began. To expedite the process and keep the components stationary on the board when soldering, one pad for each resistor and capacitor was tinned. Flux is applied before tinning for a cleaner solder joint. After each component had one side soldered to the board, the IC was next to be soldered. The IC has very small pads, so the ground pad underneath the IC was tinned and then reheated, which allowed the IC to fall into place. This kept it in place, so the IC would not move when soldering the other pads. After carefully soldering the pads of the IC, the MOSFETs were next. The same process was followed to secure and solder the MOSFETs to the board. Lastly, the inductor is soldered to the board. Due to an error in the board layout, external wires are needed to connect the inductor. 18-gauge wires are used to handle the, up to six amps, current seen through the inductor. The final soldered board is seen in figure XXXVI. The next chapter will outline the testing procedure.

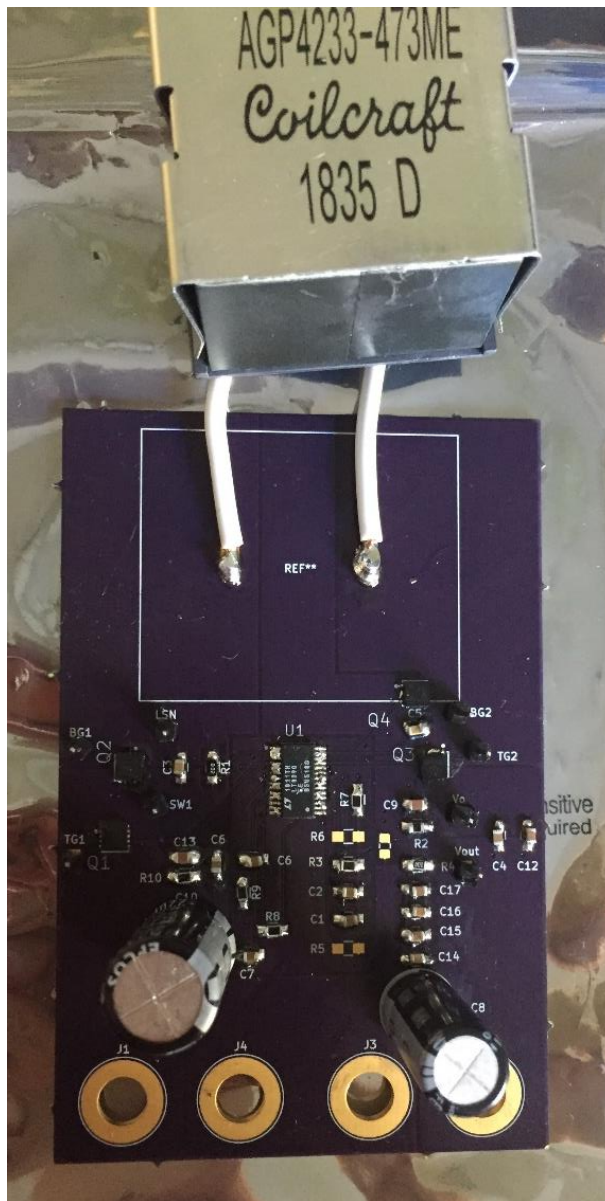


Figure XXXVI: Final soldered PCB

## Chapter 8: DC-DC Converter Testing

This chapter documents the steps and procedures for converter testing. Testing involves using an electronic load to ensure the converter functions as expected.



**Figure XXXVII:** Test setup for DC-DC Converter.

The converter initially tests low loads to prevent overheating or component damage. At high loads, the converter sees higher currents, which could possibly damage components. The BK Precision DC 8540 electronic load is set initially at 1 A and increased to 4 A in steps of 1 A. Using the RIGOL DP832 DC power supply the input voltage is initially set at 10 V and increased to 60 V in steps of 5 V. This ensures enough data points for validation. For each load, the input voltage ranges from 10-60 V. This procedure allows us to determine the efficiency of the converter at different loads.

The load and line regulation describe performance parameters of the converter that analyze converter performance. The load regulation indicates how well the converter sustains a constant output voltage at different loads. The line regulation indicates how well the converter sustains a constant output voltage at different input voltages. Equations 1 and 2 calculate the load and line regulation, and equation 3 calculates efficiency/

$$\text{load regulation \%} = \frac{V_{O\text{No Load}} - V_{O\text{Full Load}}}{V_{O\text{Full Load}}} \times 100 \quad (1)$$

$$\text{line regulation \%} = \frac{V_{O\text{Low input voltage}} - V_{O\text{High input voltage}}}{V_{O\text{Nominal input voltage}}} \times 100 \quad (2)$$

$$\text{efficiency \%} = \frac{P_{out}}{P_{in}} \times 100 \quad (3)$$

The next chapter will describe the future plans for the product and the major lessons learned.

## Chapter 9: Future Plans and Takeaways

At the end of this project, many things need extra research and further iterations to have a fully-fledged out design. The process also provided many opportunities to learn from that will help guide us through our career in the future. The main setback in this project is the limited time to design, manufacture and test the PCB. Plans to create a second revision of the PCB are in the works that would reduce clutter on the board. Thermal vias for the MOSFETs are also planned to be added to increase the efficiency of the heat dissipated by the MOSFETs. Allowing more room for extra caps on the feedback, output, and input nets would create an opportunity to add more caps without having to fabricate a whole new board. Most importantly the footprint of the inductor could be correctly mapped out, completely reducing the need for external wires.

More research into other IC's and different values for resistors and capacitors would give rise to a possible increase in efficiency, cheaper BOM, or better performance in regard to our design specifications. The project was based around the use of the LT 8390 without much research into other IC's, so looking at other ones might uncover a better performing converter. Tests including the elliptical machines would be valuable data to capture as well. Rather than using a DC power supply to generate the input voltage, the elliptical machine would provide this voltage. This testing would really put the design to the test for the desired application and see how well the simulations matched up the real-life conditions.

The most important plans for the project would be further testing of the current iteration. We ran out of time to further test and debug the circuit, which stopped us from finding the reason that the circuit was not performing to our standards. This situation caused no verifiable and quality data to be collected, and, in the end, no confirmation if the circuit that was designed worked as designed.

The main takeaway from this project, which really delayed our project in the end, was the significant amount of time simulation and PCB layout took. The simulation phase, one of the most critical phases, took considerable time to produce the results that were laid out in the design specifications. The effect of changing one component had a cascading effect on other components which made slight changes turn into large shifts in the output. After many iterations, a design that we were confident with was chosen. The PCB design process followed suit. The datasheet had many considerations to keep in mind, which are there not as suggestions, but rather informing you that the project will not work as intended if they were not followed. The process also took a considerable amount of time, longer than we had anticipated. Having little experience in designing power-based boards really slowed down the progress. More than three major iterations were done, with many minor iterations in between. If this process were to be done again, more time would be allotted to these two phases.

Some other takeaways that really made an impact were the manufacturing lead times and importance of preliminary work. A major time delay was due to the time it took from when we ordered the components and PCB to when we received them. This delayed the project at least a week and half where we couldn't do any physical testing. This delay put the project to the final days and put a considerable time pressure on us. The design work done in EE 460 set up a fantastic foundation for the design phase of the project. Having very specific and measurable design requirements really allowed the design to have no wiggle room in terms of the output and desirable metrics.

## References

- [1] D. Braun, "Braun's Senior Projects," Senior Projects, 2007. [Online]. Available: <https://courseware.ee.calpoly.edu/~dbraun/srproj.htm>. [Accessed: 19-Mar-2018].
- [2] U. Author, *60V Synchronous 4-Switch Buck-Boost Controller with Spread Spectrum Datasheet*. Linear Technologies, 2016. [Online]. Available: <http://cds.linear.com/docs/en/datasheet/8390fa.pdf>. [Accessed: 27- Feb- 2018].
- [3] R. Dominguez, A. Conejo and M. Carrion, "Toward Fully Renewable Electric Energy Systems", *IEEE Transactions on Power Systems*, vol. 30, no. 1, pp. 316-326, 2015.
- [4] A. Hilario, "ENERGY HARVESTING FROM ELLIPTICAL MACHINES USING FOUR-SWITCH BUCK-BOOST TOPOLOGY.", May 2011 [Online]. Available: <http://digitalcommons.calpoly.edu/cgi/viewcontent.cgi?article=1541&context=theses>. [Accessed: 27- Feb- 2018]
- [5] A. M. A. Gallardo, "Design and Construction of 1800W Modular Multiple Input Single Output Non-Isolated DC-DC Converters," DigitalCommons@CalPoly. [Online]. Available: <http://digitalcommons.calpoly.edu/theses/1739/>. [Accessed: 19-Mar-2018].
- [6] A. Forster, "Energy Harvesting From Exercise Machines: Buck-Boost Converter Design", 2017. [Online]. Available: <http://digitalcommons.calpoly.edu/cgi/viewcontent.cgi?article=2929&context=theses>. [Accessed: 27- Feb- 2018].
- [7] U. Author "The Green Revolution," Gyre9. [Online]. Available: <http://www.gyre9.com/portfolio-item/the-green-revolution/>. [Accessed: 19-Mar-2018].
- [8] T. Gibson, "These Exercise Machines Turn Your Sweat Into Electricity", *IEEE Spectrum*, 2011.
- [9] M. Mulrooney, "Magnetic Vs. Air Resistance Elliptical Trainers", *LIVESTRONG.COM*, 2018. [Online]. Available: <https://www.livestrong.com/article/196078-magnetic-vs-air-resistance-elliptical-trainers/>. [Accessed: 27- Feb- 2018].
- [10] D. Braun. "Soft Switching DC-DC Conversion to Harvest Exercise Machine Electricity EISG Proposal," 2010.
- [11] P. Basset, E. Blokhina and D. Galayko, *Electrostatic kinetic energy harvesting*. Wiley, 2016.
- [12] D. Briand, E. Yeatman and S. Roundy, *Micro energy harvesting*. Wiley, 2015.
- [15] R. Ford and C. Coulston, *Design for Electrical and Computer Engineers*, McGraw-Hill, 2007, p. 37
- [16] U. Author. "Electrical Engineers", Bls.gov, 2018. [Online]. Available: <https://www.bls.gov/oes/current/oes172071.htm>. [Accessed: 01- Mar- 2018].
- [17] IEEE. *IEEE Std 1233, 1998 Edition*, p. 4 (10/36), DOI: 10.1109/IEEESTD.1998.88826
- [18] United States Department of Energy. "2017 U.S. Energy and Employment Report." Department of Energy, [www.energy.gov/downloads/2017-us-energy-and-employment-report](http://www.energy.gov/downloads/2017-us-energy-and-employment-report).



- [19] Author, Unknown. "Infineon BSZ100N06LS3 Data Sheet." *Infineon BSZ100N06LS3 Data Sheet*, 2009, [www.infineon.com/dgdl/Infineon-BSZ100N06LS3-DS-v02\\_03-en.pdf?fileId=db3a30431ddc9372011ebb132c97000a](http://www.infineon.com/dgdl/Infineon-BSZ100N06LS3-DS-v02_03-en.pdf?fileId=db3a30431ddc9372011ebb132c97000a).
- [20] R. Morgan, "What Is the Average Gross Profit Margin for a Small Retail Business?", *Smallbusiness.chron.com*, 2018. [Online]. Available: <http://smallbusiness.chron.com/average-gross-profit-margin-small-retail-business-22607.html>. [Accessed: 20- Feb- 2018].
- [21] A. Sireci, "DC-DC Converter Control System for the Energy Harvesting from Exercise Machines System", 2017. [Online]. Available: <http://digitalcommons.calpoly.edu/cgi/viewcontent.cgi?article=3014&context=theses>. [Accessed: 27- Feb- 2018].
- [22] Y. Benitez Ramirez, J. Gonzalez Herrera and J. Rosero Garcia, "Technical evaluation of the electric energy production process within a distributed generation model for gyms in Colombia", *2012 IEEE International Symposium on Alternative Energies and Energy Quality (SIFAE)*, 2012.
- [23] T. Gibson, "Turning sweat into watts", *IEEE Spectrum*, vol. 48, no. 7, pp. 50-55, 2011.
- [24] U. Author. Strength Companion LLC, "Energy harvester for exercise equipment", US8888660B1, 2011.



The costs almost equal initial investment, but once the energy harvested overtakes initial device cost, the benefits outgrow the initial investment.

The project requires any gym goer to use the device which initiates energy harvesting. Production costs shouldn't exceed \$360. This number stems from conservative estimates of 100W workout, with 90% inverter efficiency, 80% DC-DC converter efficiency, and 12 hours of machine use per day for 41 weeks per year [1]. Product consumers make up of gym enthusiast and owners, specifically Cal Poly Rec Center.

With estimated 150 work project hours at \$47.41 hourly rate, the labor approximates at \$7,156. A starting engineer's hourly rate shoots close to \$47.41 according to the bureau of labor statistics [16]. This price fluctuates and may change. The actual project work hours came to 198 hours giving a total of 9,387.18. An additional elliptical machine used for previous projects provides testing purposes.

Depending on usage amount and project life cycle, the project can produce variable amounts of money. Determining the products overall revenue without a finished product to analyze. The breakeven point mentioned above, of about \$350, seems like a reasonable educated guess [1].

The product stands in testing phase, ensuing an unknown production timeline. More testing ensures product reliability, environmental responsibility, and efficiency. The product should not affect elliptical machine performance and should last the elliptical machine's lifetime. Proper converter construction and designing requires minimal maintenance.

The estimated time follows:

Time Optimistic =  $T_o = 100$

Time Most Likely =  $T_m = 150$

Time Pessimistic =  $T_p = 200$

$$Expected\ Time = \frac{T_o + 4T_m + T_p}{6} = \frac{100 + 600 + 200}{6} = 150\ hours$$

Once the project ends, two options emerge:

1. If nearly completed, production and manufacturing can start.
2. If unfinished, the project needs more testing and design revisions.

#### **4. If manufactured on a commercial basis:**

Because of the twenty elliptical machines in the Cal Poly REC center, it estimates twenty product manufacturing units for the first year. The device manufacturing cost would follow the estimate mentioned of about \$350 per device, not including the elliptical machines. Selling the device for \$500 would result in a price margin of 30%. This price margin mimics other products sold, which normally run a profit margin of 25%-50% [2]. If an elliptical machine runs for ten years before replacement, then the cost per unit time reaches fifty dollars per year.

#### **5. Environmental**

The project connects to the electrical grid. Natural resources build and run the electrical grid. The project indirectly requires natural grid power resources like coal, natural gas, fossil fuels, wind, nuclear, hydro and thermal sources. In start of harvesting coal, fossil fuels, and natural gas, species inhabiting the land forcibly evacuate and relocate, which possibly affects their ecosystem. Electronics create byproducts after their lifetime. If disposed inappropriately, the byproducts release harmful, environmental chemicals. Harming the environment directly affects humans and other species. Manufacturing and PCB fabrication use natural resources like silicon and copper.

## **6. Manufacturability**

A few manufacturing issues include metal trace tolerances when fabricating the PCB. Considering the tolerances ensures unintended PCB issues arise. If the generated heat from the controller is improperly handled, issues could arise where parts either perform unacceptably or entirely burned. PCB layout factors an important part in manufacturability. Part placement ensures product functions at maximum capacity, by reducing chip space and board size. Minimizing wire usage guarantees less noise and clean waveforms during testing.

## **7. Sustainability**

The device's purpose creates a sustainable approach in using the gym. Users can use this device knowing they contribute in a greener, more sustainable future by help powering the gym. A design improvement consideration, which may not make it more sustainable per se, would display the user's harvested energy. This would not only encourage machine usage and preference over others, and show positive environmental impacts the user develops. By directly seeing the feasibility for a decrease in energy footprint per person, this could also influence the user to live a more sustainable life outside of the gym. For example, this person could ride their bike to work, or purchase local foods to reduce their environmental footprint.

## **8. Ethical**

Ethical principlism surrounds the ethical framework behind the project. In autonomy terms, the product does not force the user product preferences over another. Choosing a product that doesn't harvest energy results as an individual choice. Regards to non-maleficence, the product has no harmful intentions to those using it. Imagine a situation where a person forces another person to use the machine against their willpower to save money. This would go against the do-no harm value and affect the autonomy of the one using it. This product also follows the beneficence principle. The product reduces environmental harm by taking wasteful energy and converting it to useful energy. Lastly, the principle of justice applies that people have the freedom to live a healthy life, so those wanting to contribute a sustainable lifestyle should have that freedom of choice.

IEEE also lays out a code of ethics that members must follow. Some IEEE guidelines have higher implications than others regarding the product. For example, honesty and realistic claims that the product functions as properly marketed. The product should produce energy as described and in no way should state any falsehoods. Another guideline accepts the criticism of the work done. If the product has criticisms, it's important to acknowledge them and then promptly address them. The last guideline addresses avoiding injury to others, their property, or reputation. The device production, in no way, should have any intended negative uses. It should only provide user benefits. If not the case, any mistakes are immediately and responsibly handled.

## **9. Health and Safety**

Delivering unused energy back to the grid stems a health and safety concern. However, following the UL and IEEE guidelines and standards ensures safety and cautionary protocols. Also, the project requires physical activity, so the operation of the elliptical machine imposes a safety risk for the user. The user could fall or tangle themselves in the rotation of the machine and cause harm to themselves or potentially others. The projects goal reuses dissipated heat from exercising machines and the person operating the machine requires a performance level above average to maximize the project's functionality. The machine does encourage a healthy lifestyle by not only providing a means of exercise and stress relieve, but it can also encourage a more sustainable life style as well.

## **10. Social and Political**

This product impacts the social and political issues regarding the environment and sustainability. Those who support the fossil fuel industry and reject climate change find the product useless, because of and unnecessary sustainability, according to those in favoring the fossil fuel industry. If one gym implemented the product this could cause gym-goers to choose the sustainable gym, which would affect the sustainable gym's revenue. It could also cause someone to not choose a gym because they use this product.

The main stakeholder in this project is the Cal Poly Rec center. The direct impact it receives is the reduction of energy costs and byproduct emissions. On the other hand, the indirect impact is the possibility of more students, or even residents of San Luis Obispo, visiting the gym which could provide more income. This could cause more congestion in the gym though, which would cause frustration on those in the gym. The project produces an inequity in the usage of certain elliptical machines, as ones with this device are used more than others causing a shortage of usable elliptical machines.

Another stakeholder is those in the surrounding environment. This product reduces the pollution in the atmosphere by replacing power plant generated energy with that of that produced by the elliptical. This replacing of energy provides a healthier environment for those living there. Billions of people around the world are inadvertently affected by how this product is developed, manufactured, and used. Seeing firsthand, the impact of pollution on the environment it's important to keep this in mind. If the trend of sustainability continues, in the limit there would be no need for coal or fossil fuel related power plants. The indirect impact would be loss of jobs and industry in the power generation sector. Over three million Americans work in this sector and many of them would be out of a job with training that may no longer be needed. [18]

## **11. Development**

Learning about the Monte Carlo technique introduced a new strategy that shows how component tolerances can severely affect the desired device output. The Gantt chart demonstrates a fantastic method that lays the project planning in an organized visual fashion. The literature search, in the references section, assisted in finding reliable, credible sources that back claims in the report. Anticipated learning outcomes include knowing how to effectively simulate a circuit, efficiently design a prototype, and build and test the product in the power sector.

## Appendix B: LTSpice Net File

This describes the .net file for the LTSpice simulation used to verify the designs.

```
*
C1 N011 0 47nF
C2 N012 0 4.7n Rser=27K Cpar=100p
V1 IN 0 60
R1 SW1 N001 2m
C3 N002 SW1 0.1μ V=100 Irms=2.1 Rser=0.0606238 Lser=0 mfg="KEMET" pn="C1210C104K1RAC"
type="X7R"
M$Q1 IN TG1 SW1 SW1 BSZ100N06LS3
M$Q2 SW1 N004 0 0 BSZ100N06LS3
R2 Vdq3 OUT 15m
C4 Vdq3 0 4.7μ V=50 Irms=15 Rser=0.00481132 Lser=0 mfg="KEMET" pn="C1210C475K5RAC" type="X7R"
C5 SW2 N003 0.1μ V=100 Irms=2.1 Rser=0.0606238 Lser=0 mfg="KEMET" pn="C1210C104K1RAC"
type="X7R"
R3 N013 0 309k
C6 N007 0 4.7μ V=6.3 Irms=0 Rser=0.003 Lser=0 mfg="TDK" pn="C2012X5ROJ475M" type="X5R"
C7 N010 0 0.47μ V=10 Irms=1.32 Rser=0.0460968 Lser=0 mfg="KEMET" pn="C1206C474K8RAC" type="X7R"
XU1 N004 N002 SW1 TG1 SW1 N001 IN N007 N006 MP_01 N010 N010 N010 Vdq3 OUT 0 N008 N011 N009
N012 N013 0 0 Vdq3 TG2 SW2 N003 N005 0 LT8390
R7 N009 0 3.24k tol=1 pwr=0.1
R8 N008 N007 100K
R9 N006 0 165K
R10 IN N006 383K
C9 Vdq3 0 1μ V=50 Irms=0 Rser=0.008 Lser=0 mfg="TDK" pn="C3225X7RIHIO5M" type="X7R"
C10 IN 0 15μ V=63 Irms=2.65653 Rser=22.1 Lser=0
C11 IN 0 4.7μ V=50 Irms=15 Rser=0.00481132 Lser=0 mfg="KEMET" pn="C1210C475K5RAC" type="X7R"
C12 Vdq3 0 4.7μ V=50 Irms=15 Rser=0.00481132 Lser=0 mfg="KEMET" pn="C1210C475K5RAC" type="X7R"
C13 IN 0 1μ V=50 Irms=0 Rser=0.008 Lser=0 mfg="TDK" pn="C3225X7RIHIO5M" type="X7R"
M$Q4 SW2 N005 0 0 BSZ100N06LS3
M$Q3 Vdq3 TG2 SW2 SW2 BSZ100N06LS3
R4 OUT N009 113k tol=1 pwr=0.1
I1 OUT 0 5.4
C14 OUT 0 4.7μ V=50 Irms=4.89 Rser=0.0139203 Lser=0 mfg="KEMET" pn="C1206C475K5PAC" type="X5R"
C15 OUT 0 4.7μ V=50 Irms=4.89 Rser=0.0139203 Lser=0 mfg="KEMET" pn="C1206C475K5PAC" type="X5R"
C16 OUT 0 4.7μ V=50 Irms=4.89 Rser=0.0139203 Lser=0 mfg="KEMET" pn="C1206C475K5PAC" type="X5R"
C17 OUT 0 4.7μ V=50 Irms=4.89 Rser=0.0139203 Lser=0 mfg="KEMET" pn="C1206C475K5PAC" type="X5R"
L1 N001 SW2 47μ Ipk=18.6 Rser=0.0028 Rpar=4427.4 Cpar=0 mfg="Coilcraft" pn="AGP4233-473"
C8 OUT 0 330μ V=63 Irms=1.42 Rser=0.049 Lser=0 mfg="Nichicon" pn="UPL1J331MRH" type="Al electrolytic"
.model NMOS NMOS
.model PMOS PMOS
.lib C:\Users\gusgu\Documents\LTspiceXVII\lib\cmp\standard.mos
.tran 30m startup
.meas Pin AVG -V(IN)*I(V1)
.meas Pout AVG V(OUT)*I(I1)
.meas Eff param Pout/Pin
;step param Iload 1 6 1
* suppress high freq \nswitching spikes
* suppress high freq \nswitching spikes
* X5R dielectrics
* X5R dielectrics
* BSC034N03IS can't handle \n36 V, look into other mosfets with low Rdson
* For resistive load, BS100N06LS3\npass 80 A current pulse, surpassing \nmosfets drain pulse current max of 80A.
* Ceramic caps should be placed\nnear regulator input & output to suppress\nhigh freq, switching spikes.
```

- \* Cin network should have low enough ESR and is sized to handle max rms current.
- \* Cin has I rms max of 3.5 A.
- \* Cout network should reduce output voltage ripple.
- \* Cout = 620u
- \* C = 120u
- \* C1=50n
- \* The input and output should have a combination of electrolytic and ceramic capacitors for effective noise filtering and to reduce ESR for minimum power loss.
- \* RT, the frequency setting resistor, should be placed close to the chip.
- \* To prevent ringing, add a small gate resistance to each MOSFET.
- \* Always choose a low ESL current sense resistor
- \* R4 = 84.5k
- \* R7 = 2.37k
- \* Changes made for update revisions:
  - changed the feedback resistor divider network
  - included actual component parameters for output and input capacitors, inductors
  - still need to include actual component parameters for the noise filtering ceramic caps, so verify all caps
- \* output current limit or inductor current limit might be the reason why loads above 5.4 A don't work.

.lib LT8390.sub  
 .backanno  
 .end  
 \*